D17

THE SPACE SHUTTLE ASCENT VEHICLE AERODYNAMIC CHALLENGES CONFIGURATION DESIGN AND DATA BASE DEVELOPMENT

Charlie C. Dill
NASA/George C. Marshall Space Flight Center
Huntsville, Alabama

J. C. Young, B. B. Roberts, M. K. Craig
NASA/Lyndon B. Johnson Space Center
Houston, Texas

J. T. Hamilton
Rockwell International Corporation
Downey, California

W. W. Boyle
Lockheed Missiles & Space Company
Huntsville, Alabama

ABSTRACT

The phase B Space Shuttle systems definition studies resulted in a generic configuration consisting of a delta wing orbiter, and two solid rocket boosters (SRB) attached to an external fuel tank (ET). The initial challenge facing the aerodynamic community was aerodynamically optimizing, within limits, this configuration. As the Shuttle program developed and the sensitivities of the vehicle to aerodynamics were better understood the requirements of the aerodynamic data base grew. Adequately characterizing the vehicle to support the various design studies exploded the size of the data base to proportions that created a data modeling/management challenge for the aerodynamicist. The ascent aerodynamic data base originated primarily from wind tunnel test results. The complexity of the configuration rendered conventional analytic methods of little use. Initial wind tunnel tests provided results which included undesirable effects from model support structure, inadequate element proximity, and inadequate plume simulation. The challenge to improve the quality of test results by determining the extent of these undesirable effects and subsequently develop testing techniques to eliminate them was imposed on the aerodynamic community. The challenges to the ascent aerodynamics community documented in this paper are unique due to the aerodynamic complexity of the Shuttle launch. Never before has such a complex vehicle been aerodynamically characterized. The challenges were met with innovative engineering analyses/methodology development and wind tunnel testing techniques.

INTRODUCTION

During first stage flight, which for purposes of this paper corresponds to the flight regime from a Mach number of 0.60 through SRB separation, aerodynamic data bases were required to support various subsystem design studies. Over-all vehicle aerodynamic characterization was required for vehicle performance analyses, vehicle structural design analyses, and SRB separation system design studies. More detailed aerodynamic inputs were required for venting analyses, protuberance design studies, tile load studies, and the ascent air data system design study. This paper discusses the aerodynamic challenges and consequent approaches/techniques to overcome them relative to the aerodynamic characterization of the Space Shuttle launch vehicle (SSLV), its four elements in proximity (orbiter, external tank, two SRBs), and the orbiter's basic components (wing, elevons, and vertical tail). Three basic challenges are addressed in terms of an ascent launch vehicle aerodynamic data base and a SRB separation aerodynamic data base.

CHALLENGE: AERODYNAMIC OPTIMIZATION OF BASIC GENERIC CONFIGURATION

The phase B Space Shuttle systems definition studies resulted in a generic launch configuration consisting of a delta wing orbiter and two solid rocket boosters attached parallel to an external fuel tank. The evolution of this generic configuration (Fig. 1) to its present form is the result of many system and subsystem optimization studies. Preeminent among these, in the early 1970's, were performance trade studies, guidance and control design studies, and attach structure sizing studies. Because vehicle aerodynamics is a basic input to these studies, the ascent aerodynamic community was initially challenged to provide a data base that would allow configuration optimization from an aerodynamic standpoint. This challenge was met by several parametric configurational studies in the early 1970's. These studies provided a data base for determining the relative aerodynamic effect of ET and SRB nose shapes, SRB location (longitudinal and radial) on the ET, and orbiter incidence relative to the ET. The significant results of these studies (Fig. 2) showed that an ogive ET nose shape produced the least

launch vehicle drag and consequently the best aerodynamic performance; that reducing the orbiter incidence to a minimum would minimize attach structure loads by reducing the orbiter longitudinal aerodynamics; and that moving the SRBs down and aft reduced launch vehicle drag, increased stability by moving the aerodynamic center aft, and minimized aerodynamic interference on the orbiter. This movement of the SRBs also reduced the probability of contact with the orbiter wing during SRB separation. In the 1975 time frame, after the major configurational changes had taken place, additional parametric drag reduction studies were conducted to support on-going performance improvement trade studies. Innovative aerodynamic fairing designs were generated (Fig. 3) and their drag reducing potential investigated. Several configurations reduced drag (Fig. 3) and consequently improved aerodynamic performance. However, weight and manufacturing cost proved too formidable thus negating their benefits.

CHALLENGE: DEVELOPMENT/MANAGEMENT OF REQUIRED AERODYNAMIC DATA BASE

The initial concept of the launch vehicle aerodynamic data base was, relative to the final product, simple. With both the Space Shuttle main engine (SSME) and SRB nozzles having gimbal capability, sufficient control authority existed to negate using aerodynamic control surfaces during ascent. The elevons could be set in a single position for the entire ascent flight regime. Element proximity aerodynamics were considered secondary inputs to the attach structure design because thrust and inertial forces were so much larger. Therefore, the fidelity of the required launch vehicle data base was considered relatively unimportant. Even though it was understood that booster separation motors (BSM) would change the aerodynamic flowfield associated with the launch vehicle at SRB separation, the degree of change was underestimated. This was primarily due to a lack of separation system requirement definition and a lack of understanding of the criticality of controlling the nonlongitudinal aerodynamic forces to ensure no recontact.

As the Shuttle program developed and the sensitivities of the vehicle to aerodynamics were better understood the requirements of the aerodynamic data bases grew. Structural loads studies of the elevon actuator and wing structure showed capability exceedances. This dictated scheduled elevon movement as a function of Mach number (Fig. 4) to maintain actuator and wing structure within allowable limits. Because trajectory parameters affecting hinge moments would vary from flight to flight, and because of the inclusion of uncertainties on the wind tunnel derived hinge moments for any set condition, an active elevon load relief system was implemented to ensure no elevon actuator overload. This elevon movement also changed the orbiter proximity aerodynamics which had now been determined to have a significant impact to the attach structure loads. Consequently, the launch vehicle aerodynamic data base now had to include the effects of elevon movement. With the realization of the acute sensitivity of the vehicle to ascent aerodynamics, particular attention now had to be paid to the fidelity of the launch vehicle data base. That is, the seemingly minor effects of the distribution between the elements of the airload on the attach structure, the asymmetry created by the ET protuberances, and the SSME/SRB plume effects on the forebody became significant. The sensitive orbiter thermal protection tiles imposed a stringent design requirement (minimized BSM exhaust plume impingement) on the SRB separation system. This dictated high BSM thrust, over a very short burn time, and a particular orientation of the BSMs (Fig. 5). Elevated thrust was required to account for the cosine losses associated with the BSM 40 deg pitch and shallow 20 deg inboard roll angles. The combination of high thrust and forward facing jets in the SRB nose frustum greatly amplified the anticipated BSM exhaust plume effect on the vehicle flowfield (Fig. 6). This placed greater emphasis on the fidelity of the data base methodology and attached more significance to the BSM plume scaling parameters, utilized for wind tunnel testing, in the data base. Naturally, with the better understanding of the vehicle's acute sensitivity to aerodynamics, coupled with questionable wind tunnel test results (to be discussed later), the uncertainties on the aerodynamic data bases also became prominent inputs to the various discipline studies. Therefore, adequate aerodynamic characterization of the vehicle to support the various design studies exploded the size/complexity of the data bases to proportions that created a data modeling/management challenge for the aerodynamicist. However, math modeling methodology which included the effects of the potential changing vehicle parameters on aerodynamics and their associated uncertainties was developed. This modeling methodology satisfied the user discipline requirements and provided adequate aerodynamic data bases for design studies.

LAUNCH VEHICLE AERODYNAMIC DATA BASE

Aerodynamics represent external applied forces to which the vehicle as a whole and its discrete structure reacts in flight. Therefore, historically, launch vehicle aerodynamic data bases are composed of two parts: a static stability data base which constitutes the resultant three aerodynamic force and three moment coefficients, and the airloads data base which is comprised of distributed localized pressure coefficients over the geometry of the vehicle. Naturally, the integration of the airloads data base into resultant forces/moments must equal the static stability force/moment data to ensure consistency between the various system design studies relative to overall vehicle design. The Space Shuttle launch vehicle aerodynamic design data base, in this respect, is no different. The uniqueness of the Shuttle data base is that five vehicles (Fig. 7) must be dealt with in a consistent fashion — the mated vehicle and its elements (orbiter, ET, LSRB, RSRB). Since each of the elements

contribute significantly to the mated vehicle aerodynamic characteristics, none can be treated as a simple protuberance with relative minor interference effects. Each must be dealt with as an independent element in proximity to others. Additionally, the data base includes aerodynamic characterization of three orbiter components — wing, vertical tail, and elevons (inboard and outboard).

In the initial planning of the launch vehicle aerodynamic data base the aerodynamicist had to consider, along with the inherent characteristics of the basic outer moldlines of the generic vehicle, the interference effects of the ET and SRB protuberances, the airloads on the attach structure and its interference effect, and the significant effect of the SRB and SSME exhaust plumes. Consideration also had to be given to the primary source of the data base — the wind tunnel. Ideally, the aerodynamicist desired to utilize a single high fidelity model to simultaneously determine both the static stability force and moments and the distributed pressures — including plume effects. This, however, was not possible due to the physical limitations/complexity of a model to obtain the data and the interference effects of the model support system required to supply the high pressure gas for the plume simulations. Early in the Shuttle program, these considerations were hampered by a lack of knowledge of how to properly simulate the plumes and the fact that few wind tunnel facilities had the capability of supplying an auxillary high pressure air supply for plume testing. Therefore, a methodology was derived to account for these considerations and work around the problems associated with generating a consistent launch vehicle data base through combination of results from different types of wind tunnel tests.

The total coefficient (Fig. 8) is comprised of forebody and base characteristics. Furthermore, the forebody coefficients are separated into plume-off (p-off) data and plume-on (p-on) increments to account for the effects of the plumes. This formulation permitted the determination of the most significant aerodynamic characteristics, the p-off forebody data, from one test (A in Fig. 8) and the plume effects from an independent test (B in Fig. 8). This minimized the model support system effects in the data base. Plume-off base environments on the models are removed from the total measured test (A) results to create p-off forebody data. These base environments are irrelevant to the data base because of the model support system interference and the overwhelming changes created by the SRB/SSME exhaust plumes. By including the forebody plume effects as p-on minus p-off increments the effect of the model support system required for plume testing (B) is reduced to a second order effect. The base characteristics are determined from the plume test. By utilizing the measured p-on base pressures from test (B) rather than p-on minus p-off increments to be applied to the p-off base environments from test (A), the model support system effects on the base characteristics are eliminated and the effects of the plumes are adequately included in the data base. The airloads data base is formulated in much the same manner. The p-off forebody pressure coefficient distributions over the geometry of the vehicle are determined independently of the p-on pressure coefficient increments and then combined. Again, with this formulation the model support system effects are minimized.

Each of the six static stability forces and moments for the mated vehicle and its four elements are formulated in this manner. The forebody coefficients are a function of the freestream Mach number, the vehicle's orientation to the freestream flow (α,β), and the elevon deflection angles (Table 1). Math modeling of the elevon effects on the mated vehicle characteristics, using a fourth order polynomial fit, has been incorporated into the data base at the request of the trajectory and guidance/control disciplines to facilitate its use. The element data are provided for nine discrete inboard/outboard combinations. Wing and vertical tail shear, bending, and torsion and elevon hinge moments constitute the component data. These are formulated similarly to the element data. The base characteristics are formulated as forces and moments primarily as a function of altitude. This is due to their first order dependency on the plume characteristics, which, for a given nozzle and engine operating characteristics, are primarily a function of altitude. However, math modeling has been incorporated to account for the small effects due to vehicle attitude and SSME power level changes. This methodology formulation allowed, early in the Shuttle program, determination of a quality data base. Then, as forebody configurational changes took place, the plume technology data base matured, and plume-on facility testing capability developed, refinements to the data base could be effected without regenerating the complete data base.

Two types of uncertainties were generated for the launch vehicle data base — tolerances and variations. These uncertainties, although not statistically derived, were generated as three-sigma incremental values with, in general, a normal distribution about the nominal data base. The tolerances, or lower uncertainty bounds, represent a measure of the experimental wind tunnel test data scatter about the established nominal data base. Tolerances were utilized in the Shuttle program for operational subsystem design. Variations, or upper uncertainty bounds, represent the potential difference between the wind tunnel derived, experimental characteristics and the actual flight vehicle characteristics. Variations were utilized in the Shuttle program as constraints in the flight planning activities. Ordinarily variations are derived by employing the historical flight experience of a vehicle similar to the one being designed. No vehicle similar to the Space Shuttle launch vehicle has ever flown. However, vehicles such as the generic lifting bodies and high altitude/high speed aircraft are similar to the reentering orbiter. The orbiter entry aerodynamic discipline utilized the flight experience of these vehicles to derive "variations" for the orbiter entry aerodynamic data base. The ascent aerodynamic community utilized the orbiter entry variation-to-tolerance ratio along with the established

launch vehicle element tolerances to establish the launch vehicle variations. Both tolerance and variation uncertainties were generated for each totally independent forebody force, moment couple, and aerodynamic center coefficient for each component and element of the launch vehicle. This permitted determination of the total moment uncertainty for each component and element as the root-sum-square (RSS) of these three independent contributors. The mated vehicle uncertainties were established as the RSS of each element's uncertainty. The base characteristic uncertainties were likewise independent and combined in an RSS fashion with the forebody uncertainties. Analytical modeling was formulated to allow assessment of a single coefficient uncertainty or any combination of coefficient uncertainties by any subsystem discipline.

SRB SEPARATION AERODYNAMIC DATA BASE

The Shuttle Solid Rocket Boosters (SRBs) are separated at burnout from the launch vehicle by means of two basic phenomena. Longitudinal separation is achieved as a result of the higher axial acceleration of the orbiter/external tank (OET). Lateral and normal separation are achieved, however, by the application of thrust to the SRBs and aerodynamic forces. Unlike previous cylindrical launch vehicles, control of these nonlongitudinal forces is critical to assure that no recontact occurs. This criticality manifested itself in the aerodynamicist's ability to model three aerodynamic phenomena: (1) the proximity effect of one vehicle's flowfield on those of nearby vehicles, (2) the jet interaction effect of the BSM plumes on the flowfield surrounding all of the vehicles, and (3) the effect of direct BSM plume impingement on the external tank. Each of these phenomena is a function of the orientation of the OET with respect to the free stream flow and the relative displacements and orientations between the vehicles. The jet interaction and plume impingement effects are also a function of a plume scaling parameter. This knowledge defined the set of eight independent parameters, the effects of which had to be considered in deriving the separation data base (Fig. 9). The effects of Mach number and Reynolds number were found to be second order in the range of anticipated flight conditions and were thus included in the data base uncertainty. To preclude the necessity of updating the complete data base each time the vehicle outer moldline was changed, the dependent variables (aerodynamic coefficients) were formulated as BSM plume-on and plume-off proximity increments; that is, coefficient increments to be added to SRB and OET free-stream aerodynamic data. Utilizing this approach would allow the effects of minor configuration changes to be adequately reflected in updates to the isolated aerodynamics with negligible effects on the proximity increments.

It became obvious that the use of eight independent variables in the data base would present severe difficulties if a standard square grid of representation was utilized in modeling the required aerodynamic characteristics. The most obvious difficulty would be the number of data points required. The squareness of the grid in 8-dimensional space would also assure that most of the data points would be far removed from areas of interest. In fact, many data points would be required in locations that are unrealizable due to physical constraints imposed by the basic configuration. Obviously, superimposing the large matrix of proximity variables required at a large ΔX on $\Delta X = 0$ would be unrealizable since the $\Delta X = 0$ position constitutes the mated position of the SRB's where the other variables can only have the value of zero. As with the launch vehicle data base, consideration also had to be given to the wind tunnel, the basic source of the aerodynamic data. Limitations on specific combinations of the independent parameters ΔX, ΔY, ΔZ, $\Delta\alpha$, $\Delta\beta$ were imposed by physical constraints of the facility and its model mounting/sting movement capability.

These difficulties were circumvented by developing a unique data organization concept to handle the five proximity independent variables. This new approach, designated the "hypercube" format, allows data to be placed only along required separation paths. At each desired ΔX two 4-dimensional hypercubes are situated so as to encompass anticipated dispersions in ΔY, ΔZ, $\Delta\alpha$, and $\Delta\beta$. An outer cube encompasses all dispersions, including system failures, while an inner cube includes the nominal separation path with 3σ dispersions. These hypercubes are not constrained to have parallel opposite sides to that they can be shaped to match physical constraints imposed by the test facility and still provide data near the required trajectory points as determined by trajectory dispersion analyses (Fig. 10). Data points were generated at the vertices of the hypercubes. In addition, an interior point is placed within each hypercube to increase the data density in a region of interest. Typical BSM plume-on SRB trajectories through the hypercube matrix are demonstrated in Figure 11 in terms of the parameters ΔX, ΔY, and ΔZ. The ΔX values at which hypercubes are placed were selected to maintain constant time increments at the separation relative longitudinal acceleration rather than constant length increments. This increases the data density early in the motion when trends are being established.

The use of this approach has provided a much higher data density along separation trajectory paths while reducing the required number of data points by a factor of at least 20 from a square grid. A special algorithm has been developed which transforms these 4-dimensional arbitrary shapes into 4-dimensional cubes so that a low order polynominal can be easily fit to the vertices and interior point, thus providing interpolation. Interpolation in the remaining independent variables α, β, and the plume scaling parameter is handled in a similar manner, although the organization of these variables is based initially on 3-dimensional cubical shapes since there are no physical interference constraints to be taken into account.

The uncertainties associated with the SRB separation aerodynamic data base are composed of three components: an error resulting from the hypercube interpolation process, an error due to the asymmetry of the motion of the two SRBs with respect to the OET, and an error associated with scaling the BSM plumes. The uncertainty component associated with interpolation error accounts for the inability of the hypercube interpolator polynomials to exactly model the data and for the fact that the data base was generated at a constant value of Mach number. It also implicitly accounts for the random uncertainty associated with the wind tunnel data measurements/acquisition system. The uncertainty component associated with asymmetric SRB motion accounts for the error incurred in performing all plume-on testing with the SRB's in symmetric positions with respect to the OET. SRB asymmetry modifies plume-on aerodynamics by establishing unequal impingement of the BSM plumes on the external tank and by causing an asymmetric interaction of the plumes with the free-stream flow. The third aerodynamic uncertainty component results from errors in plume scaling, that is, errors incurred by using the jet-to-free stream momentum ratio rather than the momentum flux ratio as the plume simulation parameter (discussed later). The total coefficient uncertainties in the data base were obtained by root-sum-squaring the contribution of these three components.

CHALLENGE: WIND TUNNEL TESTING TECHNIQUES/IMPROVEMENTS

The primary sources of the Space Shuttle ascent aerodynamic data base are wind tunnel test results. The multibody configuration with its significant interrelated interference effects precluded using conventional analytical tools to characterize the vehicle. Initial wind tunnel tests provided results which included effects from model support structure, inadequate element proximity, and inadequate plume simulation. It became obvious, as the Shuttle program matured, that these undesirable effects were significant. The challenge to improve the quality and detail of test results by determining the extent of these effects, and subsequently develop testing techniques to eliminate them, was imposed on the aerodynamic community. In the process of establishing the ascent aerodynamic data base two basic types of wind tunnel test results were utilized. Force and moment data were obtained by using balances located in the models. Data of this type were obtained for the mated vehicle, the elements, and the components for the launch vehicle data base. Data of this type were also obtained for the SRBs and OET combination in proximity for the SRB separation data base. The other type of data obtained from testing were local pressure distributions (airloads test) over the entire vehicle. These data were obtained by locating pressure orifices on the outer moldline of the model and recording the sensed pressures. These data were utilized in formulating the airloads for the launch vehicle data base. As mentioned earlier, the physical limitations/complexity of the models did not permit simultaneously obtaining all the required data with a single model/test. Therefore, different type tests were conducted and their results combined to generate the data base. Mated vehicle/element plume-off force/moment and airloads test results were combined with plume-on mated vehicle/element airloads test results to obtain the launch vehicle data base. The SRB separation data base utilized only BSM plume-on and plume-off force-moment test results. Associated with each of the above type tests were peculiar generic problems and inadequacies that had to be resolved in order to establish a quality data base.

LAUNCH VEHICLE/ELEMENT/COMPONENT PLUME-OFF TESTS

Initial emphasis was placed on the mated vehicle force/moment aerodynamic characterization. To support generating the required data, wind tunnel tests utilizing a single sting support (Fig. 12) were conducted. The elements were rigidly mounted to each other with scaled attach structures thus preserving the required proximity. A single balance was located in the orbiter which measured the six aerodynamic forces and moments required by the launch vehicle data base. This single sting/base mounting arrangement was most practical and provided minimum sting effects on the forebody aerodynamic data.

As the Shuttle program matured emphasis shifted to defining the element and component aerodynamic characteristics. Wind tunnel tests, designated as IA81 and IA135, were conducted in the Ames Research Center Unitary Plan Wind Tunnel (ARC UPWT) to provide aerodynamic data supporting the integrated vehicle baseline characterization cycles 1 and 2 (IVBC-1 and IVBC-2). These tests, to obtain data for each of the elements and components in proximity, utilized a four-sting model support system (Fig. 13). Each element, which contained a balance for measuring the aerodynamic forces and moments, was mounted on a separate sting in proper proximity with the free-stream air off. The sting and balances were designed to minimize deflections considering model weight and aerodynamic load, yet, provide adequate measurement accuracy in terms of the expected aerodynamic loads on the model. However, with freestream air on the aerodynamic loading on each element caused excessive model separation. Thus, the proper interference effects of the elements on each other was not realized. And, furthermore, each element was at a different attitude relative to the freestream flow. Additionally, the presence of the ET sting and the sting support created an effect on the forebody aerodynamics. The presence of these effects was implicitly determined when the summation of the element did not equal the mated vehicle data obtained from other tests utilizing a single sting support system. The presence of these effects was further verified by a series of parametric tests conducted in the Marshall Space Flight Center's 14-in. Trisonic Wind Tunnel. The significance of these undesirable effects, except from a purist standpoint, were of little consequence to the aerodynamist. However, as structural load sensitivity studies developed,

significant impacts of small changes in the element/component aerodynamics on the vehicle's attach structure, wing design, and vertical tail design were realized. Obviously, the undesirable effects in the aerodynamic data base needed to be eliminated if possible, rather than incorporate them into uncertainties on the data.

To eliminate the above undesirable effects the ascent aerodynamic community and wind tunnel model designers established the "shell model" concept for Space Shuttle testing (Fig. 14). This concept offered two distinct advantages over previous model designs: (1) only a single sting support is required, thus eliminating the majority of the sting interference effects, and (2) permits measuring the element data simultaneously with the mated vehicle data, thus ensuring that the summation of the element aerodynamic data equals the mated vehicle aerodynamic data. This is achieved by utilizing a balance in each element and specific attachment of the element's outer moldline (OML) shells to each other via the scaled attach structures. This permits each balance to measure aerodynamic loads experienced by certain combinations of elements (i.e., the SRB balances measure SRB aerodynamics, the ET balance measures ET and SRB aerodynamics, and the orbiter balance measures the mated vehicle aerodynamics). Thus each element's aerodynamic characteristics are obtained directly through measurement (SRBs) or by subtracting appropriate balance results (orbiter and ET). This shell model concept was pilot tested using a 1 percent scale model in the ARC UPWT, and later utilized with a 2 percent model (Fig. 15) in the 16T Propulsion Wind Tunnel facility at the Arnold Engineering Development Center (AEDC) to provide a large part of the power-off data base for STS-1.

To eliminate the remaining potential sting interference effects on the orbiter forebody aerodynamic characteristics an additional model was designed utilizing the "shell model" concept (Fig. 16). This 3 percent scale model was supported by two stings through the base of each SRB and utilized a single balance in the orbiter to determine the orbiter aerodynamic characteristics. The orbiter was mounted as a shell model to the ET/SRB combination via the scaled attach structure. This model was also utilized to determine the power-off pressure distributions on the vehicle. The orbiter balance was removed and the complete vehicle instrumented with approximately 1,500 pressure orifices. This model was also tested at the AEDC 16T facility and the results constitute the remaining part of the power-off data base for STS-1.

LAUNCH VEHICLE/ELEMENT/COMPONENT PLUME-ON TESTS

Early in the Shuttle program it was anticipated that the exhaust plumes from the SSME/SRB engines would affect the aerodynamic characteristics of the vehicle. This was based on the history of rocket-powered launch vehicles and the resulting plume effect phenomena that was developed over the years. This phenomena is philosophically demonstrated in Figure 17. For a given engine/rocket motor operating at a fixed altitude and Mach number the exhaust plume phenomena vary with increasing rocket engine chamber pressure. The plume diameter is initially too small to significantly alter the forebody pressure. Thus, the primary effect is the entrainment of the base flow by the high velocity gases in the boundary of the plume and the subsequent reduction of power-off base pressure. As the plume grows in size, it begins to block the base and increase the base pressure. Ultimately, the boundary layer will separate, and a recirculating pattern will develop. For multiple engines, the plumes will impinge upon each other and deflect exhaust flow into the base. Three or more engines can reverse enough mass into the base to choke the volume enclosed by the engines. The effect of the plumes can actually increase base pressure above the power-off level.

To simulate the plumes and their effect in wind tunnel testing the ascent aerodynamics community had three basic design options available: (1) hot gas by combustion, (2) cold or warm/heated gas, and (3) solid body simulators. Hot gas testing was eliminated as a viable option when cost and complexity were considered. Additionally, the data quality for hot gas testing is limited extensively because of the short-duration of steady state flow. The use of a solid body simulator was also eliminated from consideration. Since the base environment was not known before testing, the configuration of the plume shape could not be determined to enable design of the solid body. Historically, cold gas testing had been used almost exclusively for launch vehicle plume simulation. A cold gas model can continuously be operated to obtain 70 to 100 data points per shift in the test facility. Therefore, the Space Shuttle Program Office chose this technique to determine launch vehicle plume effects because of cost and schedule effectiveness.

In 1972, NASA initiated the planning phase for the first wind tunnel test of the Space Shuttle launch vehicle (SSLV). At this time, the technical archives were surveyed to determine the appropriate rocket exhaust simulation techniques. The data accumulated through experience with the Saturn launch vehicle were chosen for study. A comparison of the wind tunnel predictions with the Saturn flight data indicated a deficiency in the technology at that time. The base drag was substantially overestimated by the predictions from wind tunnel testing. The surveys concluded that the simulation techniques and the simulation parameters were not well understood. Therefore, the aerodynamic community was challenged to better understand the flow phenomena and develop a set of simulation parameters for use in wind tunnel testing of the Space Shuttle launch vehicle. To this end a plume technology program was initiated by NASA.

The objective of the technology program was to determine a set of functions that would correlate base pressure data generated by wind tunnel cold gas tests with full scale flight base pressure. An empirical data base was obtained using generic models with some geometry variations to assess configuration effects on the base pressure. The key independent variables were simulated gas, nozzle geometry, and geometric configuration. Hot, warm, and cold gases were used. Simulated model nozzle area ratios and nozzle lip angles varied from test to test, assuring that internal geometry was not an explicit contributor to the correlation functions. The external configurations consisted of cone or ogive noses and cylindrical afterbodies with single or triple nozzle bases (SRB and orbiter bases respectively); and, a triple body configuration to assess the effects on a centerbody (similar to the external tank on the Space Shuttle). Because difficulties were encountered in correlating the plume technology test data due to limited variations in nozzle geometry and test conditions, analytical tools were utilized to supplement the data base.

The substantial empirical and analytical data base generated throughout this technology program was then analyzed for correlation by plotting the base pressure data as a function of reasonable candidate simulation parameters. The successful simulation parameters were those that would coalesce the base pressure data to a simple function of the assumed simulation parameter. As the technology program developed, the plume simulation correlation parameters matured from the simple parameters defining plume shape to a function based on shape and gas dynamic characteristics. The final simulation parameter developed through the technology program has the form:

$$\frac{M_j \, \delta_j}{M_{e_x}{}^{a} \, \gamma_j{}^{b}}$$

This final "winning" set of simulation parameters is demonstrated in Figure 18 along with a definition of terms. The caveat, however, is that neither the hot gas technology test nor the hot gas analytical data agree with this simulation. In other words, this simulation correlated the cold/warm gas data but an apparent temperature function, $(T_c/T_{t_\infty})^c$, needed to be included to fully correlate the data. These data came too late to impact any Space Shuttle testing prior to the first flight due to program schedule and resource restrictions. However, indications were that the exclusion of the temperature function would result in an overprediction of the flight base drag and, consequently, an underestimate of vehicle performance resulting in a conservative design. The current status of the technology program is best described as "terminated incomplete." The technology program, however, yielded substantial knowledge on how to correlate the cold gas base pressure and, therefore, advanced the state-of-the-art.

Not only did the definition of the simulation parameters have to be addressed, but also the application of the required simulation in the wind tunnel had to be established. Unfortunately, the key to the technique of base pressure correlation is that the simulation parameters are a function of the base pressure itself. For example, δ_j and M_j are dependent on the Prandtl-Meyer expansion at the nozzle lip and, therefore, proportional to the base pressure and the square root of the base pressure, respectively. Consequently, if the base pressure is not known a priori, the correct simulation in the wind tunnel is impossible to establish. The technique that evolved from the plume technology program and the early SSLV tests to circumvent this problem is as follows:

1. Model nozzles are designed, using analytical tools, to provide a range of similarity parameters for a test.

2. For a fixed Mach number, a variation of the base pressure is obtained through a variation of the model's SSME and SRB chamber pressures via the auxillary high pressure air supply.

3. The variation of the base pressure from the wind tunnel test is plotted as a function of the simulation parameter. See curve A in Figure 19.

4. A similar curve can be analytically derived for the full scale prototype by assuming a base pressure (curve B, Fig. 19). This curve represents the loci of possible values of the similarity parameters for the prototype as a function of base pressure.

5. Where the curve of prototype possibilities is equal to the wind tunnel test data, the similarity is matched, and the resulting base pressure is the design value.

The SSLV test data were acquired in the ARC UPWT. This facility developed the capability to supply secondary air flow at a rate of 1500 psi and 80 lb/sec for Shuttle propulsion system simulation. In Figure 20 the model is shown installed in the UPWT 11-ft test section. Note the model support structure required to supply the high pressure air for plume simulation and an enclosure for the instrumentation

leads from the model. As mentioned earlier, this support structure, due to its interference effects on the forebody, dictated that only incremental effects of the plumes could be utilized. Balances were utilized in the orbiter wing, elevons, and vertical tail to provide incremental force/moment data for the components. Additionally, the entire vehicle was instrumented with pressure orifices to provide the incremental plume effects on the pressure distributions. The results from this type test were combined with plume-off data, determined from other tests, providing a complete plume-on launch vehicle data base.

SRB SEPARATION TESTS

Basic wind tunnel testing of separating bodies was recognized as a complex operation early in the Shuttle program. In fact, if the bodies have significantly different flight path angles, wind tunnel testing cannot be performed to adequately simulate the combined flowfield of the bodies. This is because the wind tunnel, with its inherent axial flow, provides only a single fixed flight path angle for all bodies. The addition of booster separation motor (BSM) plume simulation further complicated the testing by providing a high energy disturbance to the flowfield. Fortunately, the SRB flight path angle was not significantly different from the Orbiter/ET flight path angle during the initial phases of separation. Therefore, the error in attitude and consequent flowfield development was small and represented no stumbling block to SRB separation testing. However, determining the correct BSM plume simulation to provide the required vehicle flowfield and plume impingement effects on the OET represented a challenge to the aerodynamicist.

The requirement of correct BSM simulation manifests itself in the need to simulate the near-field jet interaction (JI) effects on the SRB aerodynamic characteristics, and the need to simulate the far-field spacial content of the plume (jet) impingement forces on the OET (Fig. 21). Early in 1973 the planning for the first SRB separation test was initiated. At this time a literature survey was conducted to retrieve all possible information relative to the effects of jet emission normal to freestream flow. The results of the survey indicated that the similarity parameter for near-field simulation of a transverse firing single jet was the ratio of jet-to-freestream momentum flux, $\bar{q}_j/\bar{q}_\infty$. Plume interaction with a freestream crossflow, as depicted in Figure 22, was then defined by the following empirical relationship for Mach disk height:

$$h_{MD} = \left[\frac{2\left(1+\frac{\gamma_j-1}{2}M_j^2\right)}{\gamma_j^2 M_j(\gamma_j+1)}\right]^{0.25}\left[\frac{1.25(1+\gamma_\infty)\gamma_\infty M_\infty^2}{(1-\gamma_\infty)+2\gamma_\infty M_\infty^2}\right]^{0.5}\left[\frac{\bar{q}_j}{\bar{q}_\infty}\right]^{0.5}\left(\frac{d_j}{(1+\cos\theta_j)}\right)$$

The far-field jet impingement pressure similarity parameters were, intuitively, momentum flux ratio and plume diameter at the point of impingement some distance from the jet (Fig. 22).

It was also found that plume gas temperature and molecular weight affect jet/flowfield interaction by strongly influencing the external flow separation distance upstream of the nozzle for low molecular weight or high temperature transverse jets. This effect is correlated by the "RT" ratio as follows:

$$\tau = \frac{(RTo)j}{(RT)_\infty} = \frac{(To/MW)j}{(T/MW)_\infty}$$

"RT" simulation provided the rationale for using air as the injectant gas in wind tunnel plume testing. Findings from the survey indicated that "RT" effects are negligible for $\tau < 7$. Since the values for flight ($\tau = 2.91$) and test with air ($\tau = 4.6$) are below this limit, unheated air was selected to simulate the BSM exhaust product plume.

Even though these similarity parameters were developed from single jet data, they were utilized for the multijet case in the early phases of SRB separation testing. At this stage of separation system development, the BSM configuration was four motors in line rather than abreast as shown in Figure 5. The forward motors were located further aft (SRB forward skirt) and the rear motor exit planes pointed toward the orbiter body flap rather than in an aft direction. Their angular orientation directed the plumes more toward the orbiter than the final configuration shown in Figure 5 (i.e., 30 deg and 20 deg rather than 20 deg and 40 deg, respectively). Results from these tests indicated significant flowfield changes and impingement pressures on the sensitive orbiter TPS tiles. To verify and expand the findings, analytical tools were utilized to reproduce the test generated plume characteristics and a separation motor technology program was initiated at the Marshall Space Flight Center. The technology program verified the simulation parameters and added insight into the relationship between the flowfield of single jets and mutliple jets. Utilizing the developed analytical tools, sensitivity studies were

performed for various alternate BSM configurations and orientations in an effort to relieve the impingement effects on the orbiter. The final BSM orientation (Fig. 5) resulted from these studies. Along with the relocation/orientation of the BSMs their thrust was increased and burn time decreased. This reduced the time that the massive complex jet/flowfield interaction would take place and still provide adequate impulse to the SRB to avoid recontact.

As plans for testing of the final BSM configuration developed, it was realized that scaling $\overline{q}_j/\overline{q}_\infty$ was no longer possible. The increased thrust required a plume gas air supply pressure (1500 psi) that exceeded the facility's capability and the small nozzle sizes required (1/32-in. throat diameter) became prohibitive. As a result, jet-to-freestream momentum ratio (ϕ_j/ϕ_∞) was selected over $\overline{q}_j/\overline{q}_\infty$ as the plume scaling parameter. This choice preserved the geometric scaling of h_{MD} but removed any dependence on nozzle size, d_j:

$$h_{MD} = \left[\frac{2\left(1+\frac{\gamma_j-1}{2}M_j^2\right)}{\gamma_j^2 M_j(\gamma_j+1)}\right]^{0.25}\left[\frac{1.25(1+\gamma_\infty)\gamma_\infty M_\infty^2}{(1-\gamma_\infty)+2\gamma_\infty M_\infty^2}\right]^{0.5}\left[\left(\frac{4S_{REF}}{\pi}\right)\left(\frac{\phi_j}{\phi_\infty}\right)\right]^{0.5}\left\{\frac{1}{1+\cos\theta_j}\right\}$$

Using momentum ratio scaling, nozzle throat size was doubled to minimize the chance of nozzle plugging (a problem encountered in early testing) and the chamber pressure was reduced to within plant gas supply limits. Model nozzle area ratio was adjusted to obtain a good match of plume cross-sectional area and hence proper simulation of the blockage associated with flowfield interaction effects. Utilizing the momentum ratio similarity parameter induced errors into the wind tunnel test results. However, an estimate of the uncertainty in SRB aerodynamic characteristics was appropriately evaluated by comparing test and flight data available from a military missile which utilized a transverse jet for attitude control. These uncertainties were included in the separation aerodynamic data base.

All testing used to define the SRB separation aerodynamic data base was conducted in the U.S. Air Force Arnold Engineering Development Center/Von Karman Facility Tunnel "A" using a 1 percent scale model of the Space Shuttle vehicle. This facility was selected because of its efficient captive trajectory system (CTS) which provides rapid computerized movement of models in the tunnel without interrupting the primary tunnel air flow.

In BSM plume-on testing, the orbiter/ET was placed on the CTS sting and the two SRBs were placed on a specially designed screw-jack adapter to the primary sting. This adapter allowed automatic movement of the SRBs in the yaw plane but required manual placement in pitch. The BSM plume-on test installation is shown in Figure 23a. Separate lines were provided to supply plume air to plenum chambers for the forward and aft nozzle clusters in each SRB. The forward clusters were fed by air flowing through the balances. Care was taken to balance the plenum chamber pressures between forward and aft jets and between left and right SRBs by means of orifice meters in the individual supply lines. In plume-on testing, previous experience has shown that it is necessary to account for SRB-to-SRB BSM plume induced flow interference as well as for the mutual coupling of the SRBs plume interference effects on the flowfield surrounding the OET. Hence, the use of both SRBs is required.

In plume-off testing, a single SRB was mounted on the CTS and moved through the hypercube matrix of points representing relative positions and attitudes of the SRB with respect to a fixed OET. The model installation is shown in Figure 23b. Although forces and moments were measured on both models, axial force and rolling moment were not measured on the SRB. The SRB model was equipped with a flow-through balance for use in plume-on testing making it impossible to measure axial force with any degree of accuracy. Rolling moment was also eliminated from the balance readings since it is negligible as a result of SRB body symmetry. Previous plume-off test experience indicated that SRB-to-SRB effects are minimal and that SRB effects on the orbiter/ET are additive, thus justifying the use of a single SRB test procedure.

The final SRB separation verification test was conducted at AEDC in March 1982 and provided the data for the current data base. This test culminated a complex wind tunnel test program to define the aerodynamics associated with SRB separation.

CONCLUDING REMARKS

The challenges to the ascent aerodynamic community documented in this paper are unique due to the aerodynamic complexity of the Shuttle's ascent flight. Never before has such a complex vehicle been aerodynamically characterized.

The initial optimization challenge was met by providing a parametric aerodynamic data base which allowed configuration optimization from an aerodynamic standpoint.

The challenge to aerodynamically characterize the vehicle with math modeling methodologies to support vehicle design and flight planning studies was innovatively met. Techniques for combining the results of several wind tunnel tests were developed which minimized model support system effects in the launch vehicle data base. A unique and effective modeling approach was developed to handle the large and complex SRB separation aerodynamic data base.

The challenge to develop testing techniques to improve the quality of initial wind tunnel test results was successfully met. Parametric wind tunnel tests and analyses were conducted to determine model support system effects on vehicle aerodynamics. The resulting optimum models and support system were designed and utilized. Comprehensive plume technology programs were conducted which established simulation parameters permitting the use of high pressure air to simulate engine exhaust plumes and high energy forward facing jet effects.

The unique and innovative engineering approaches/techniques developed to meet the aerodynamic challenges imposed by the complex Shuttle configuration and ascent flight have resulted in quality aerodynamic data bases. The success of the Shuttle ascent aerodynamic development program is exemplified by the successful STS program.

REFERENCES

1. Craig, M. K., NASA JSC; and Dresser, H. S., Rockwell International Corp.: Shuttle Booster Separation Aerodynamics. NASA Langley Research Center's Shuttle Lessons Learned Conference. 1983.

2. Roberts, B. B. and Wallace, R. O., NASA JSC; and Sims, J. L., Georgia Institute of Technology-Huntsville, AL: Plume Base Flow Simulation Technology. NASA Langley Research Center's Shuttle Lessons Learned Conference. 1983.

3. Hamilton, J. T., Rockwell International Corp.; Wallace, R. O., NASA JSC; and Dill, C. C., NASA MSFC: Launch Vehicle Aerodynamic Data Base Development and Comparison with Flight Data. NASA Langley Research Center's Shuttle Lessons Learned Conference. 1983.

4. Space Shuttle Aerodynamic Design Substantiation Report, Vol. 2 - Launch Vehicle. Rockwell International Publication SD74-SH-0206, Vol. 2K. February 1980.

SYMBOLS

A	Area
C	Coefficient
d	diameter
h_{MD}	Jet Mach disk height
M	Mach number
MW	Molecular weight
R	Universal gas constant
q	Dynamic pressure
S_{REF}	Reference area
T	Temperature
α	Angle-of-attack
β	Angle-of-sideslip
γ	Ratio of specific heats
δ	Initial expansion angle of gas
θ	Lip angle
Δ	incremental value
ϕ	Momentum

SUBSCRIPTS

A	Axial force
B	Base; bending moment
C	Chamber
E	Exit
e	Elevon
f	Forebody
H	Hinge moment
i	Inboard elevon
j	Plume boundary
l	Rolling moment
m	Pitching moment
n	Yawing moment
N	Nozzle
O	Outboard elevon
P	Pressure
S	Shear force
t	Torsion moment
V	Vertical tail
W	Wing
Y	Side force
x,y,z	Displacement of SRB from mated position
(∞)	Freestream

SUPERSCRIPTS

a,b,c	Undetermined exponents, functions of geometric configuration

TABLE 1: LAUNCH VEHICLE AERODYNAMIC DATA BASE FORMULATION

TYPE OF DATA	FORMULATION
MATED VEHICLE FOREBODY STATIC STABILITY	o MACH = 0.6, 0.8. 0.9, 0.95, 1.05, 1.10, 1.15, 1.25, 1.40, 1.55, 1.80, 2.2, 2.5, 3.5, 4.5 o α/β = $-8° \rightarrow +4°/-6° \rightarrow +6°$, $\Delta = 2°$ o ELEVON SETTINGS = MATH MODELED VIA 4TH ORDER POLYNOMIAL FIT OF DATA VARIATIONS WITH INB'D & OUTB'D SETTINGS.
ELEMENT FOREBODY STATIC STABILITY (ORB, ET, LSRB, RSRB)	o MACH = SAME AS ABOVE o α/β = SAME AS ABOVE o ELEVON SETTINGS = 9 DISCRETE INB'D/OUTB'D COMBINATIONS FOR EACH MACH.
COMPONENT STATIC STABILITY (WING, ELEVONS, V. TAIL)	SAME AS FOR ELEMENTS
POWER-ON BASE FORCE/MOMENT (ORB, ETC, LSRB, RSRB)	o ALT = $0 \rightarrow$ = 200,000 FEET o MATH MODELING INCLUDED TO ACCOUNT FOR α/β AND SSME POWER LEVEL EFFECTS
ELEMENT/COMPONENT PRESSURE DISTRIBUTIONS	o SAME AS FOR ELEMENTS/COMPONENTS ABOVE o $C_p = f(x,y,z,\phi)$

CONFIGURATION	VEHICLE	ORBITER		EXTERNAL TANK	SOLID ROCKET BOOSTERS
		LOCATION AND INCIDENCE	DESIGN EFFECTS	SIZE AND NOSE SHAPE	SIZE, LOCATION AND NOZZLE DESIGN
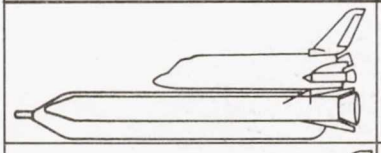	ATP (3/4/72)	•972 IN. AFT OF ET NOSE •−1.2° INCID.	• STRAIGHT WING T. E.	•318 IN. DIA. •30° NOSE CONE	•156 IN. DIA. •SRB NOSE FWD. OF ET SHOULDER •LARGE CANT NOZZLE •NO TVC
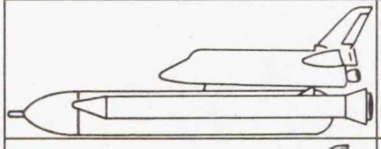	PRR (10/24/72) MCR 0026	1063 IN. AFT OF ET NOSE +0.5° INCID.	• ASRMS REMOVED • OMS PODS MOVED TO SHOULDER • SWEPT T. E.	•304 IN. DIA. •OGIVE NOSE W/RETRO PKG.	• 162 IN. DIA •SRB NOSE AT ET SHOULDER •PRE−CANT REDUCED •TVC ADDED
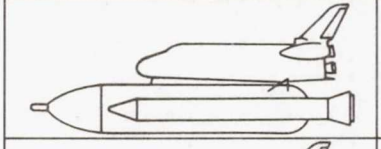	2A (12/22/72) MCR 0074	•768 IN. AFT OF ET NOSE	• INCREASED NOSE RADIUS	•324 IN. DIA.	•142 IN. DIA. • SRB AFT OF ET SHOULDER • REDUCED AFT SKIRT FLARE • NO PRE−CANT
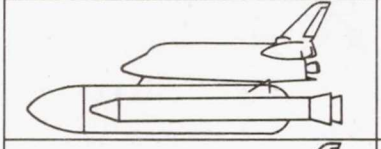	3, 3A MCR 0200 (5/73)	• 680 IN. AFT OF ET NOSE	• REDUCED WING INCID. • BODY 38 IN. SHORTER • DECREASED NOSE RADIUS	•324 IN. DIA. •REMOVED RETRO	• 142 IN. DIA. • DECREASED AFT SKIRT SIZE • 7:1 NOZZLE • INLINE SEP. MTRS.
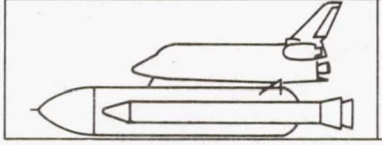	4, 5 MCR 3570		• BLUNT OMS PODS • UNCOVERED RCS PORTS	•333 IN. DIA. •BICONIC AADS	• ATTACH RING AREA REDUCED • ELIMINATED 2 OF THE 4 HOOP STRESS RINGS • 4 ABREAST SEP MTRS.

Figure 1. Space Shuttle Design Evolution.

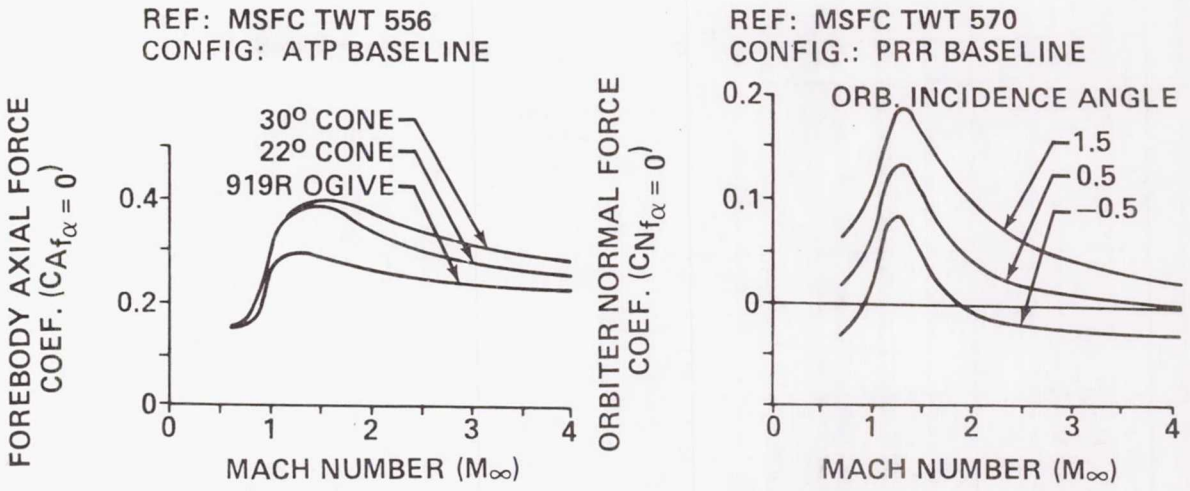

(a) EFFECT OF ET NOSE SHAPE ON LAUNCH VEHICLE AXIAL FORCE

(b) EFFECT OF ORBITER INCIDENCE ANGLE ON ORBITER NORMAL FORCE

S_{ref} = 2690 FT^2
ℓ_{ref} = 1328 IN.
MRP = ORB. NOSE ON ET CENTERLINE

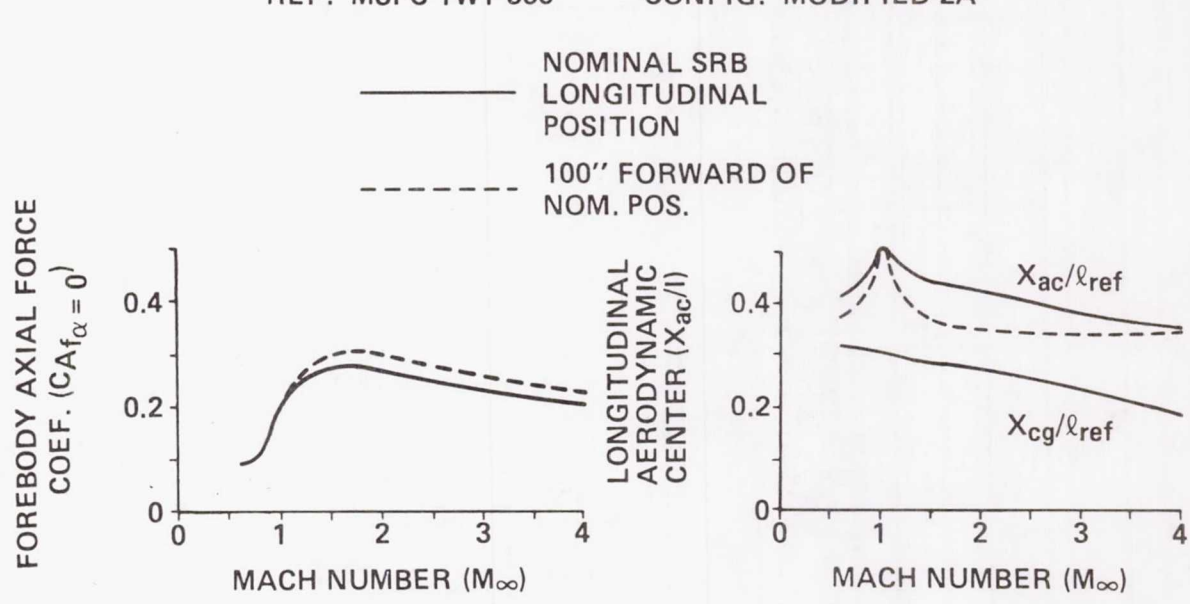

(c) EFFECT OF SRB LONGITUDINAL POSITION ON LAUNCH VEHICLE AXIAL FORCE

(d.) EFFECT OF SRB LONGITUDINAL POSITION LAUNCH VEHICLE PITCH STABILITY

Figure 2. Typical Results of Parametric Configurational Studies.

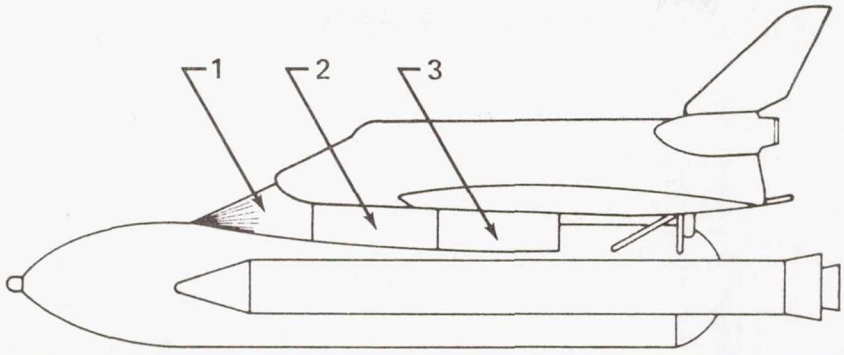

MACH NUMBER		.6	.9	1.2	3.48	4.96
% DECREASE IN FOREBODY DRAG	1	−1.0	−2.3	−1.6		
	1, 2	0	−1.0	1.3		
	1, 2, 3	9.4	7.5	5.9		

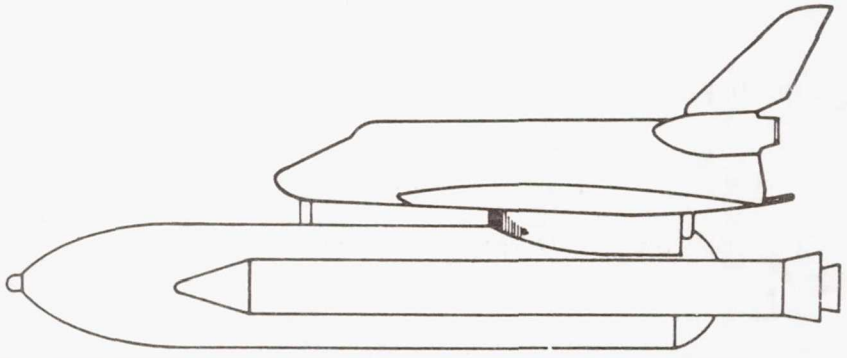

MACH NUMBER	.6	.9	1.2	3.48	4.96
% DECREASE IN FOREBODY DRAG	9.9	5.5	3.0	−1.0	0

REF: MSFC TWT 589

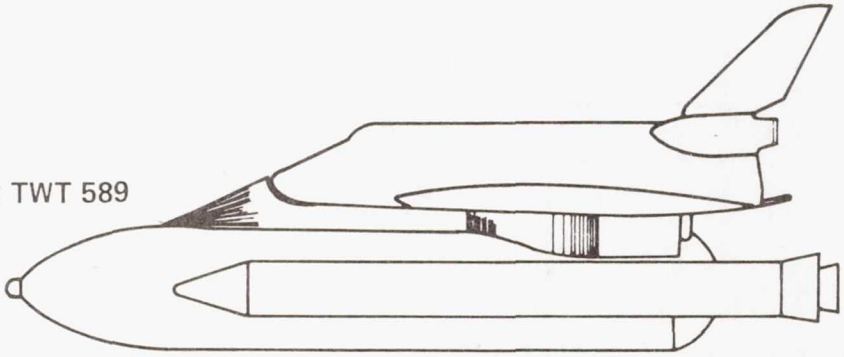

MACH NUMBER	.6	.9	1.2	3.48	4.96
% DECREASE IN FOREBODY DRAG	14.0	7.6	5.8	3.8	2.1

Figure 3. Aerodynamic Fairing Concepts for Launch Vehicle Drag Reduction.

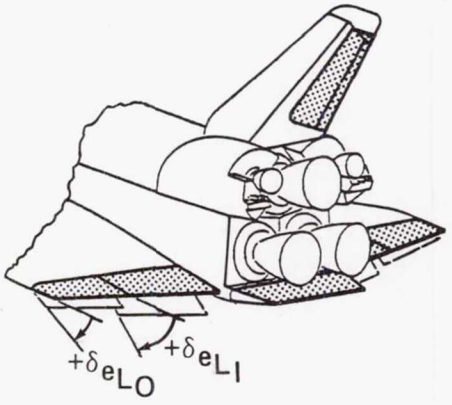

(a) SIGN CONVENTION

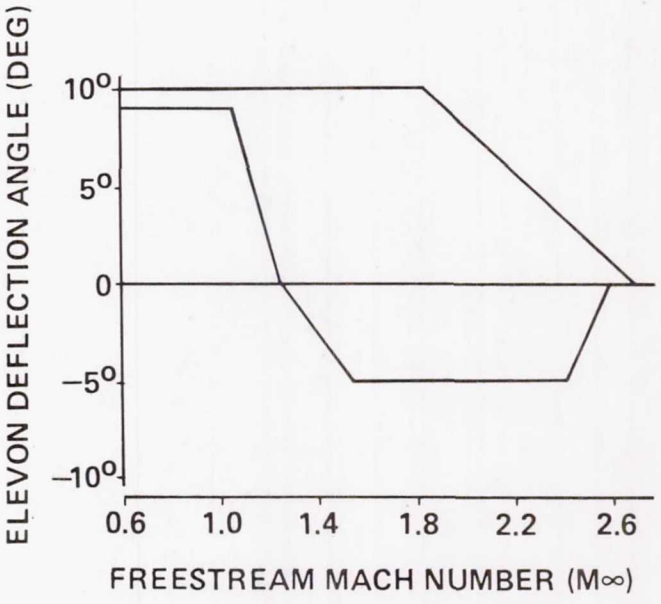

(b) ELEVON DEFLECTION SCHEDULE

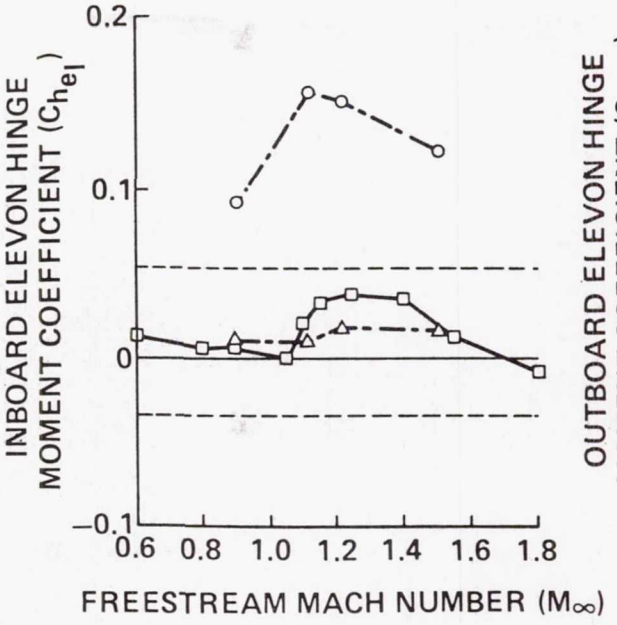

(c) INBOARD HINGE MOMENT COEFFICIENT

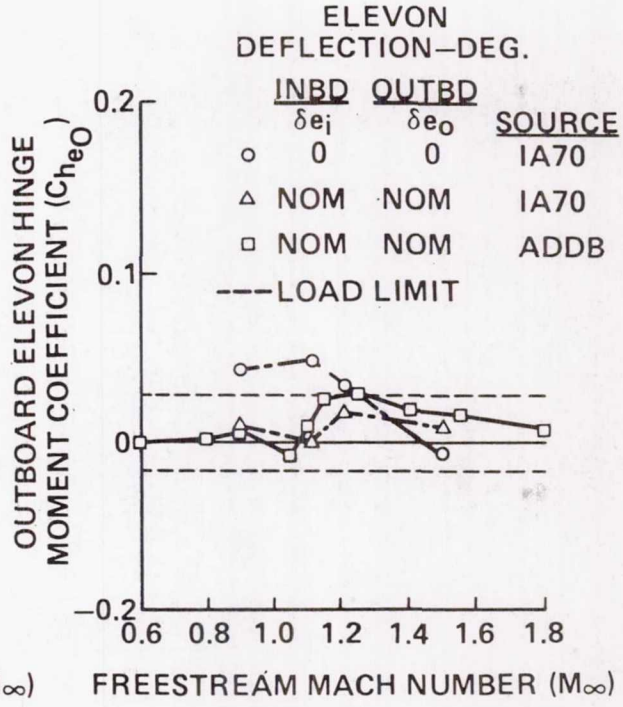

(d) OUTBOARD HINGE MOMENT COEFFICIENT

Figure 4. Ascent Elevon Deflection Schedule Requirement.

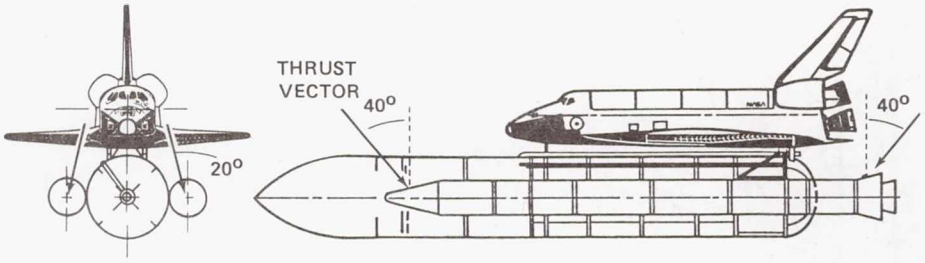

- FOUR BSMs FORWARD AND FOUR AFT
- PERFORMANCE
  - WEB ACTION TIME ~ 0.68 SECONDS
  - VACUUM THRUST/MOTOR ~ 21,000 POUNDS
  - AVERAGE OPERATING PRESSURE = 1700 PSI

Figure 5. Booster Separation Motor Orientation.

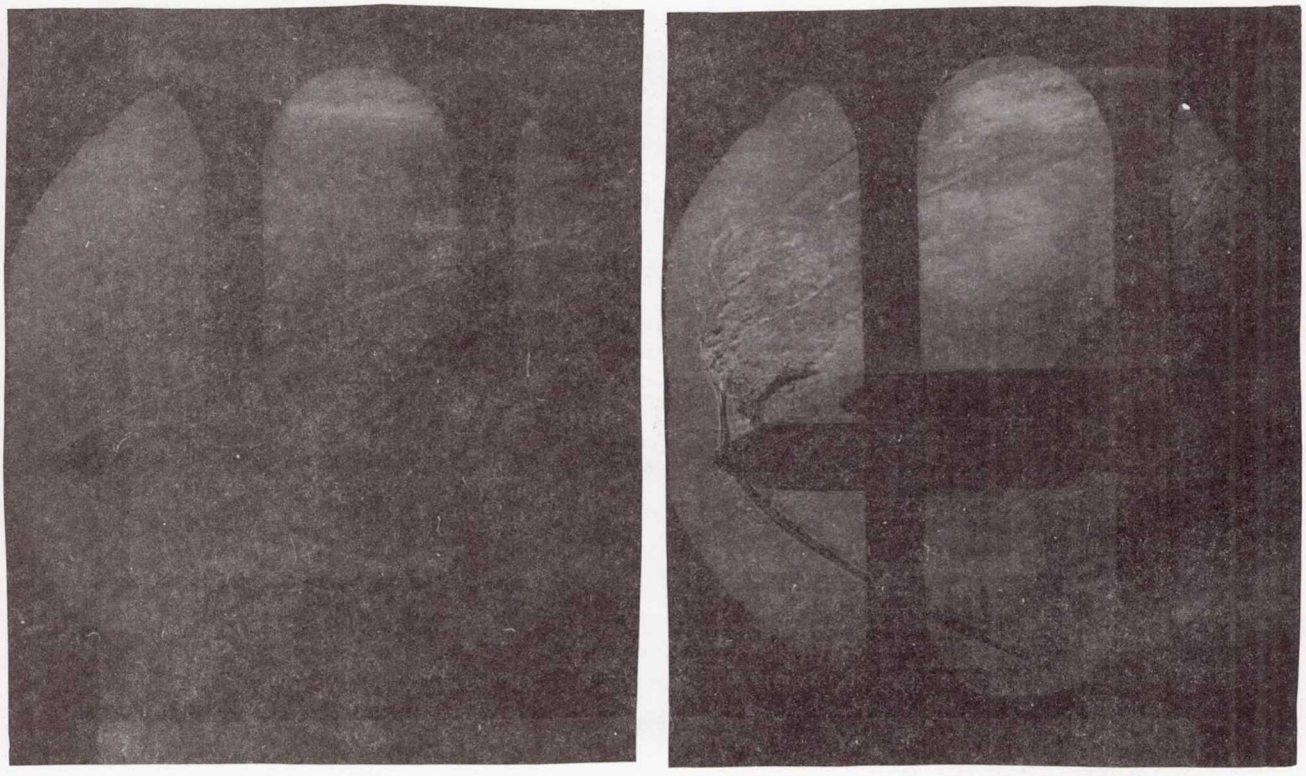

(a) BSM-Off (b) BSM On

Figure 6. Effect of BSM on Shuttle Flowfield, M_∞ = 4.5, AEDC/VKF Tunnel A.

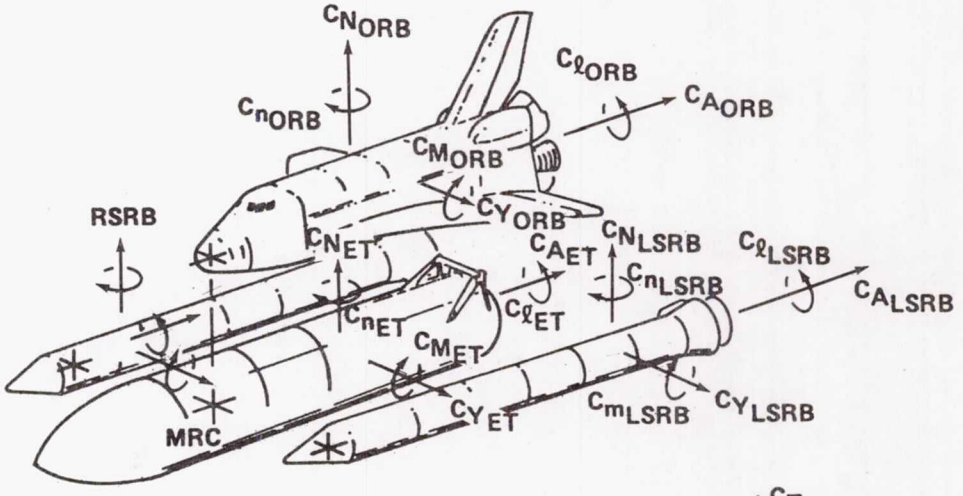

ELEMENT STATIC STABILITY

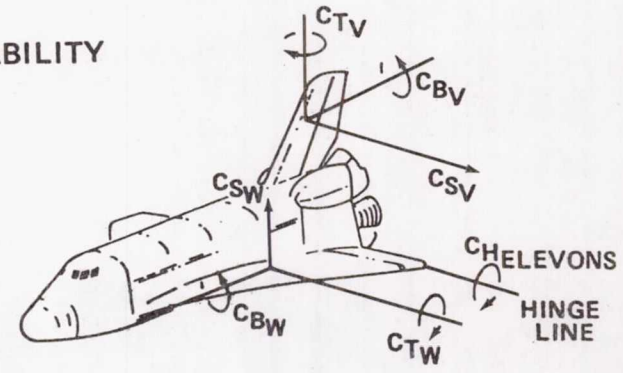

COMPONENT STATIC STABILITY

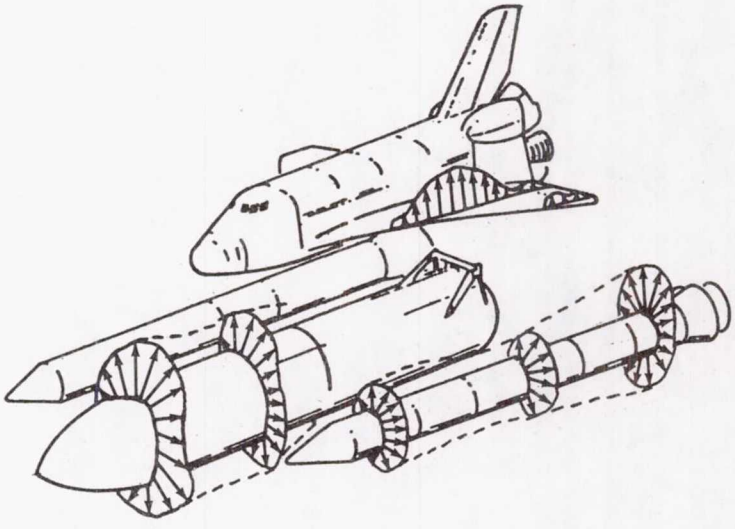

PRESSURE DISTRIBUTIONS (AIRLOADS)

Figure 7. Launch Vehicle Aerodynamic Data Base.

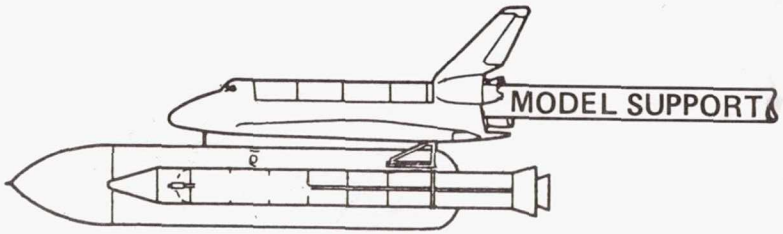

WIND TUNNEL TEST Ⓐ

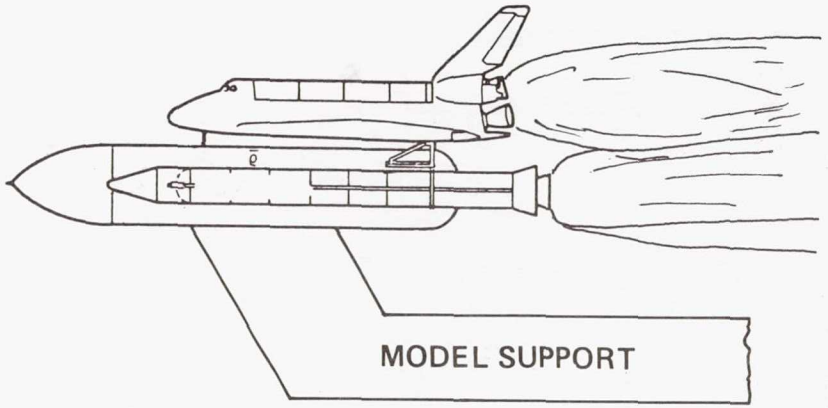

WIND TUNNEL TEST Ⓑ

IN GENERAL,

$$C_{X_{TOTAL}} = \left(C_{X_{f_{P-OFF}}} + \Delta C_{X_{f_{DUE\ TO\ PLUMES}}}\right) + C_{X_{BASE\ P-ON}} + C_{X_{FOREBODY\ P-ON}}$$

$$C_{X_{f_{P-OFF}}} = \left(C_{X_{TOTAL}} - C_{X_{BASE}}\right)_{P-OFF}$$

Ⓐ

$$C_{X_{BASE\ P-OFF}} = \frac{1}{gS_{ref}} \int (P_B - P_\infty)\, d\,(A_B)$$

Ⓐ

$$C_{X_{B_{P-ON}}} = \frac{1}{gS_{ref}} \int_{P-ON} (P_B - P_\infty)\, d\,(A_B)$$

Ⓑ

$$\Delta C_{X_{f_{DUE\ TO\ PLUMES}}} = \frac{1}{q\,S_{ref}} \int (P_{P-ON} - P_{P-OFF})\, d\,(A)$$

Ⓑ

Figure 8. Aerodynamic Coefficient Formulation.

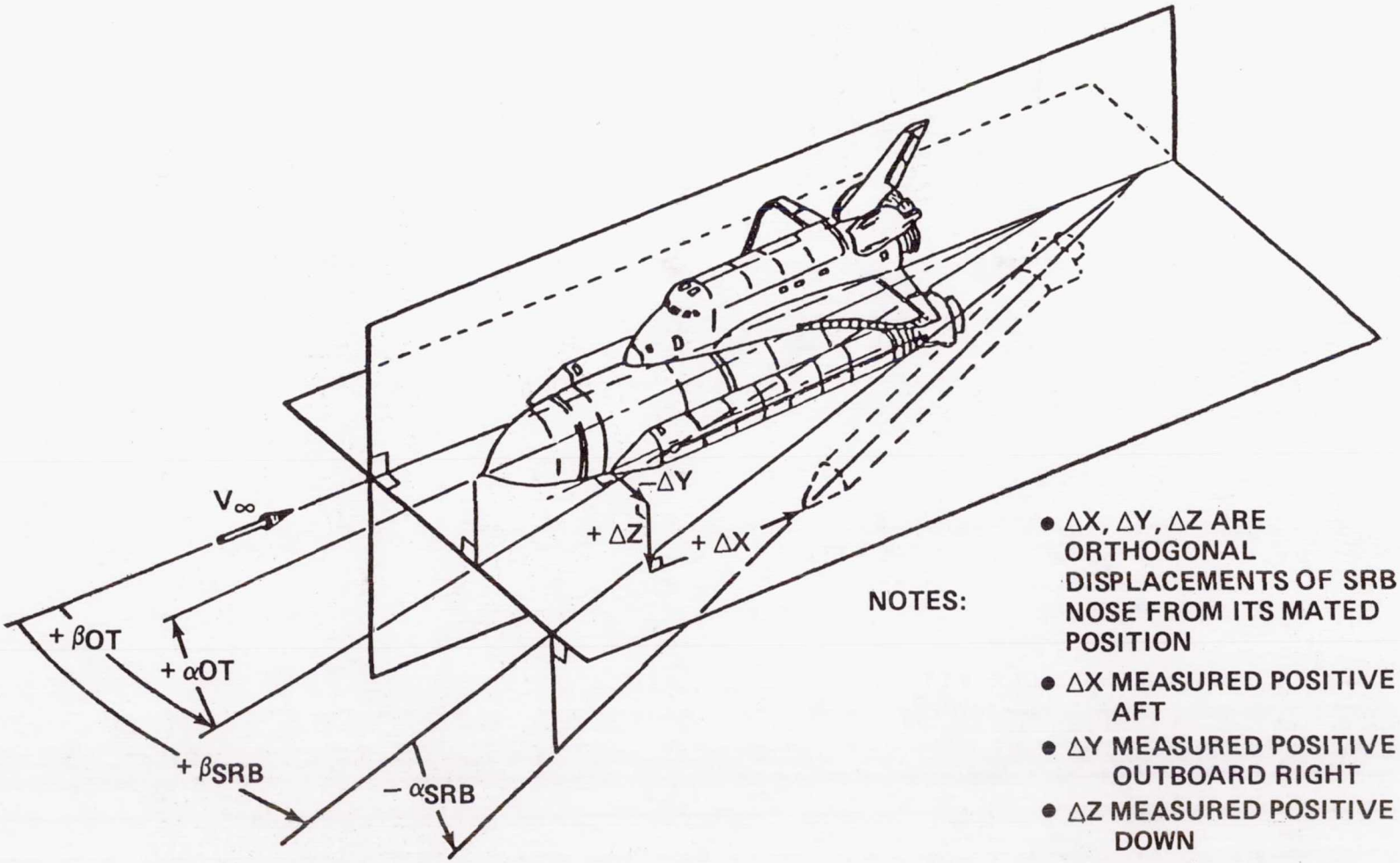

NOTES:

- $\Delta X, \Delta Y, \Delta Z$ ARE ORTHOGONAL DISPLACEMENTS OF SRB NOSE FROM ITS MATED POSITION
- ΔX MEASURED POSITIVE AFT
- ΔY MEASURED POSITIVE OUTBOARD RIGHT
- ΔZ MEASURED POSITIVE DOWN
- $\Delta\alpha \equiv (\alpha_{SRB} - \alpha_{OT})$
- $\Delta\beta \equiv (\beta_{SRB} - \beta_{OT})$
- SEPARATION MOTOR JET–TO–FREESTREAM MOMENTUM RATIO IS ALSO INDEPENDENT VARIABLE

Figure 9. SRB Separation Aerodynamic Independent Variables.

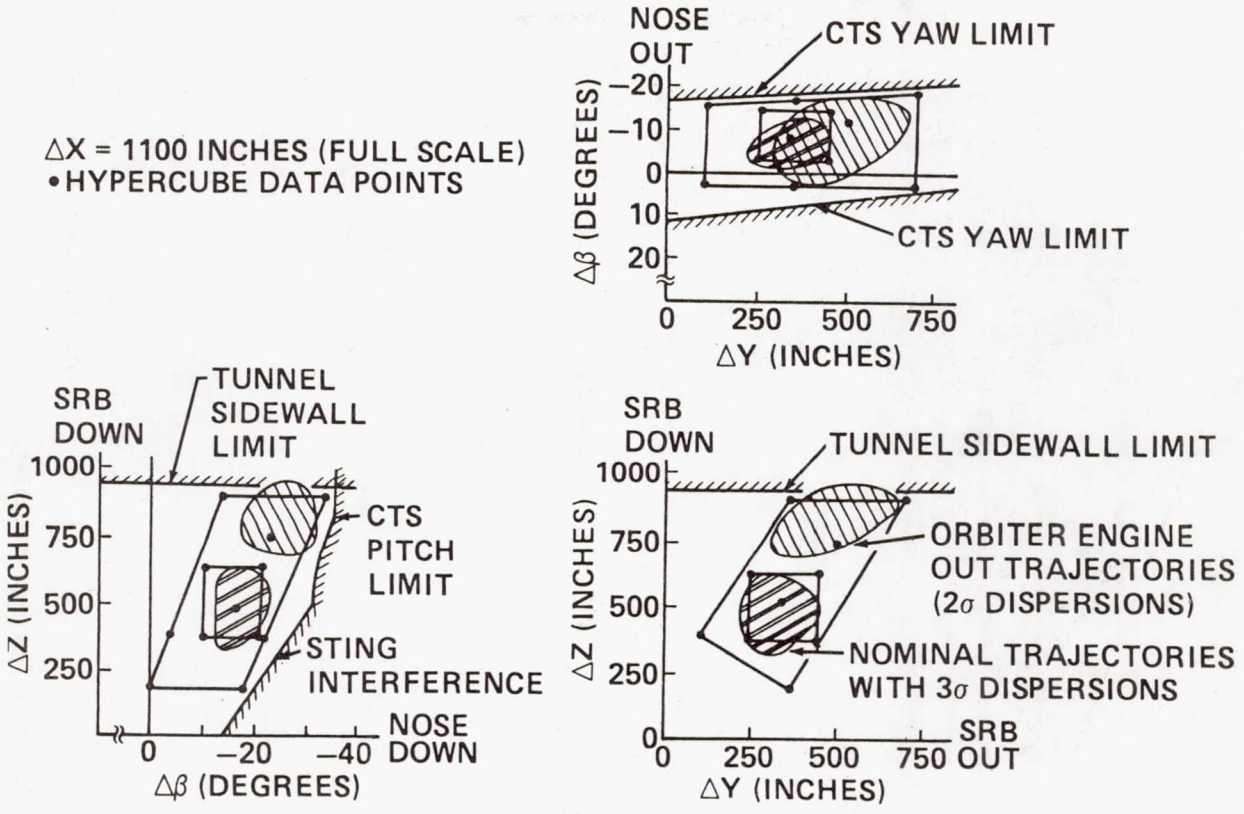

Figure 10. Trajectory Envelope Cross Section.

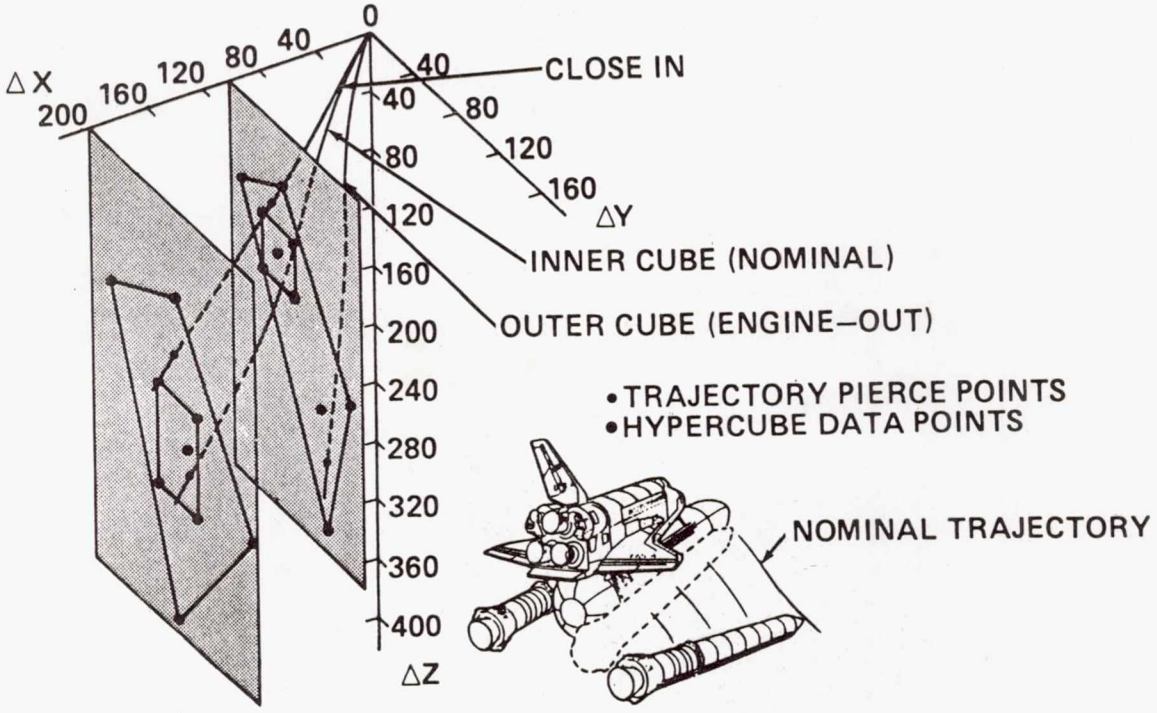

Figure 11. Typical SRB Separation Trajectories Through Hypercube Matrix (BSM Plume-On).

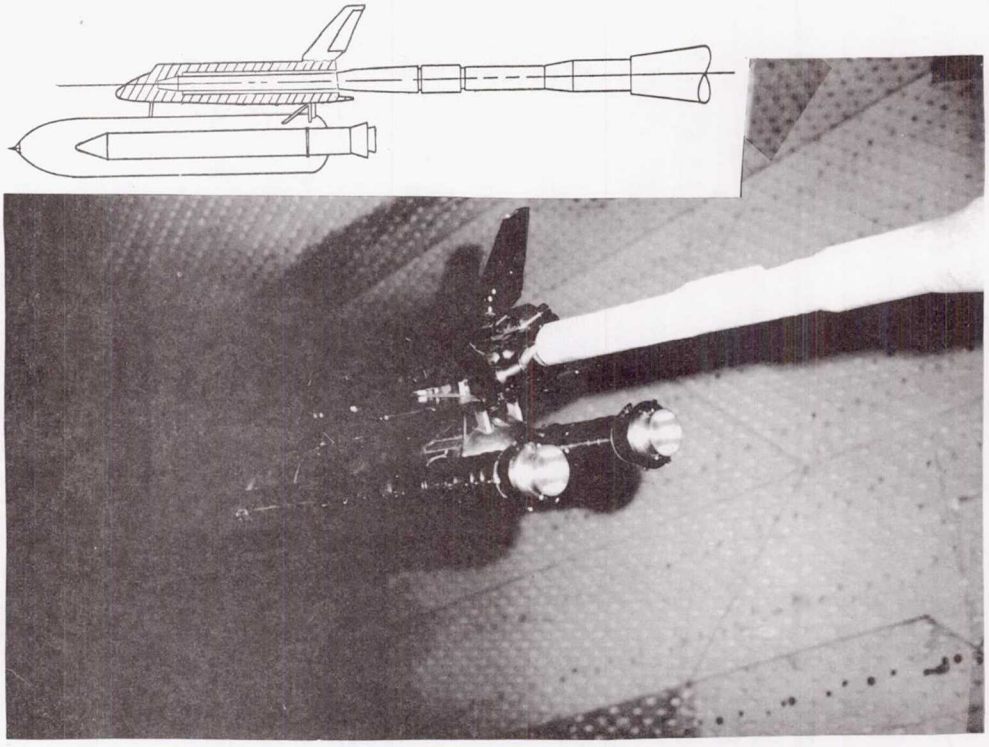

Figure 12. Single Sting/Single Balance Mounting Arrangement.

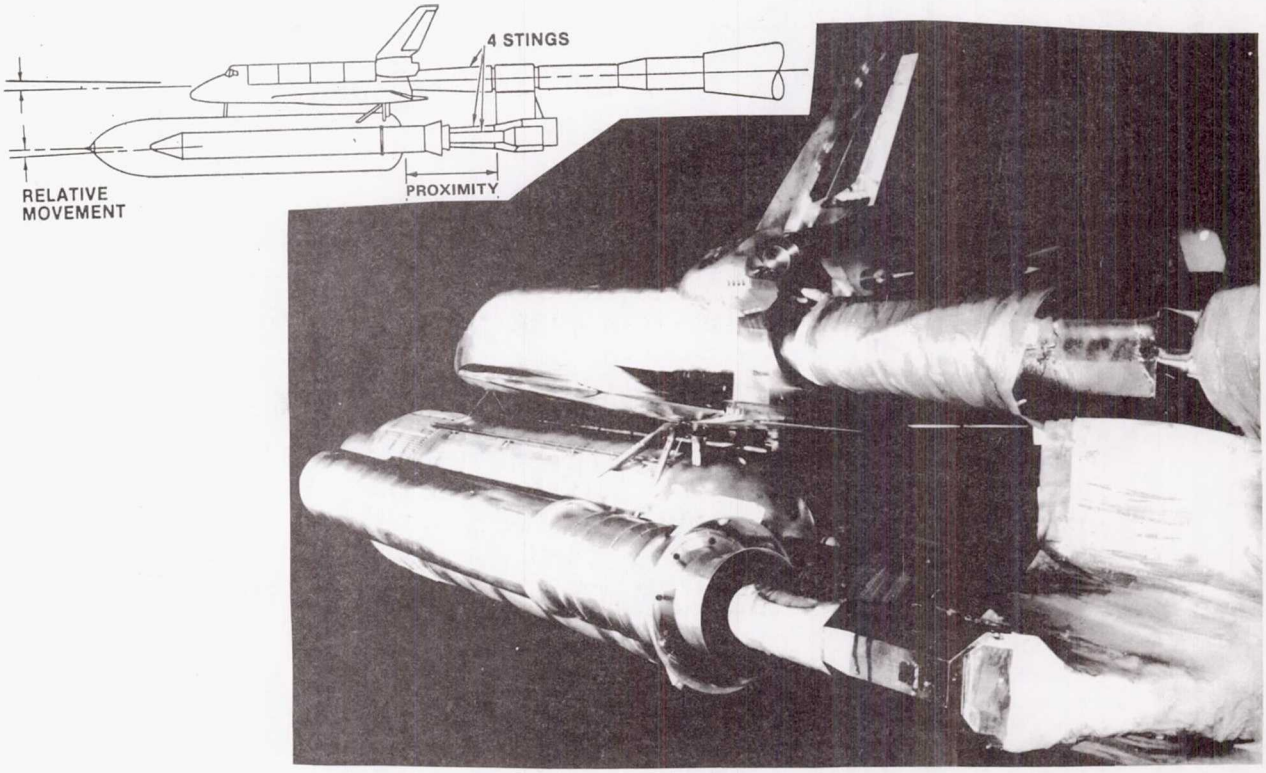

Figure 13. Model Support System for Early Element Tests.

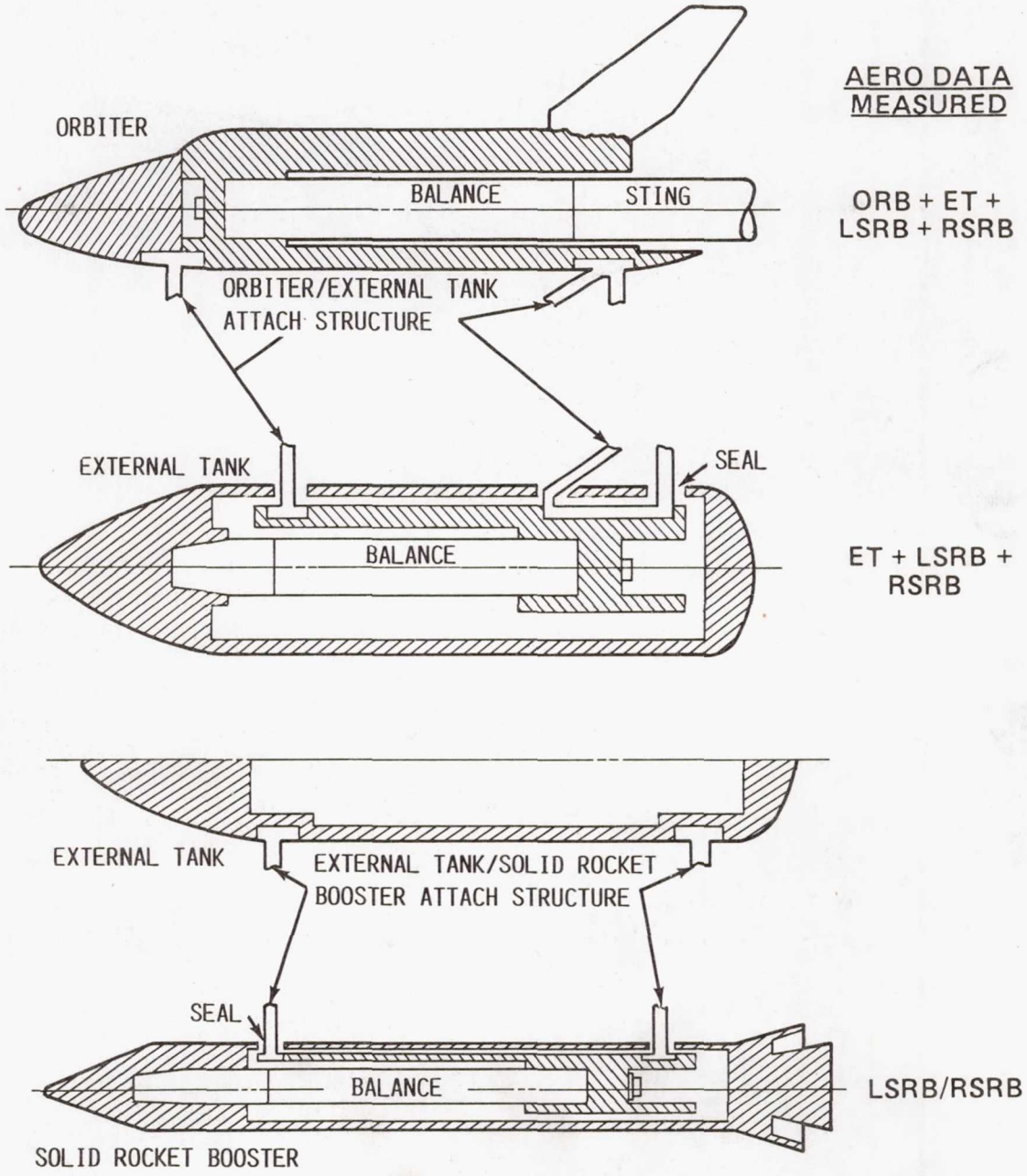

Figure 14. Single Sting/Multiple Balance "Shell Model" Concept.

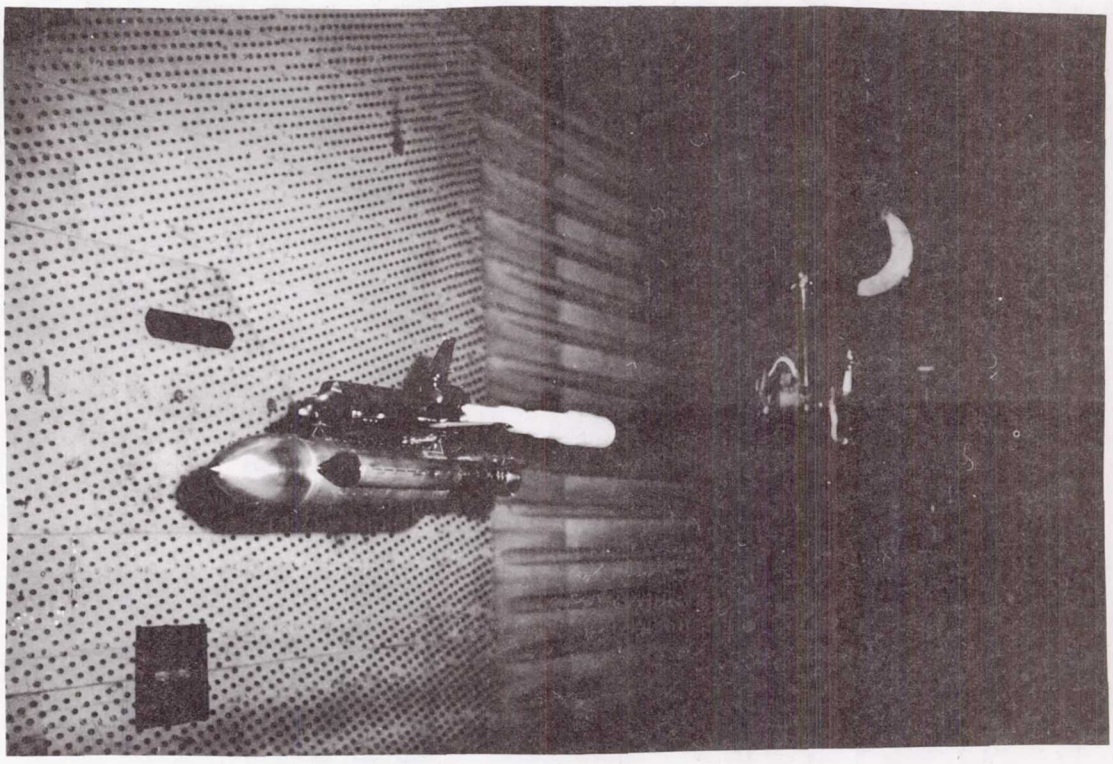

Figure 15. Single Sting/Multiple Balance Shell Model in AEDC 16T Tunnel.

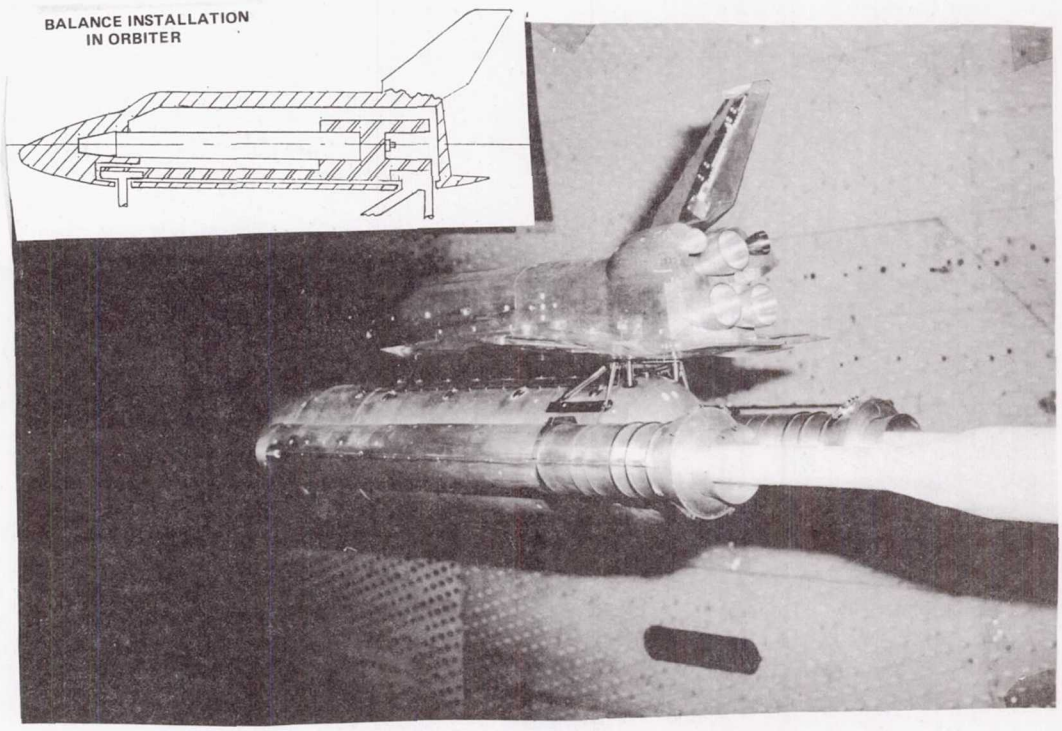

Figure 16. Dual Sting/Single Balance Shell Model in AEDC 16T Tunnel.

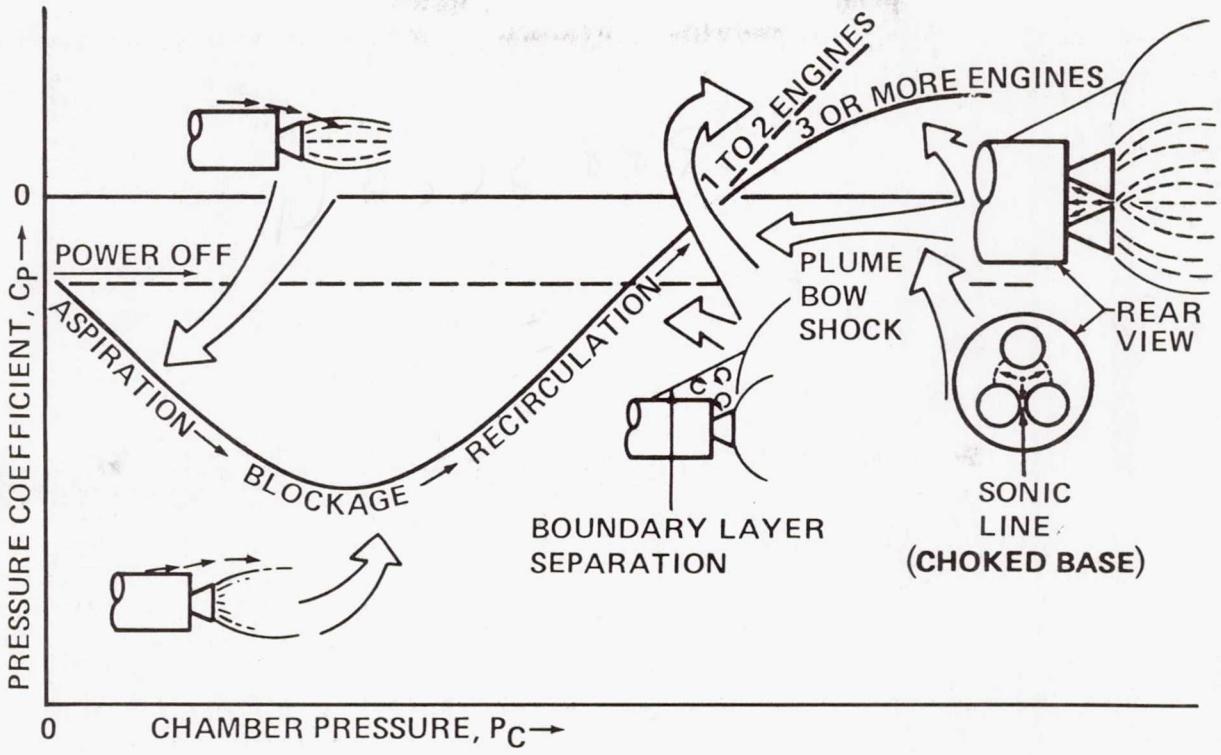

Figure 17. Base Flow-Exhaust Plume Phenomena.

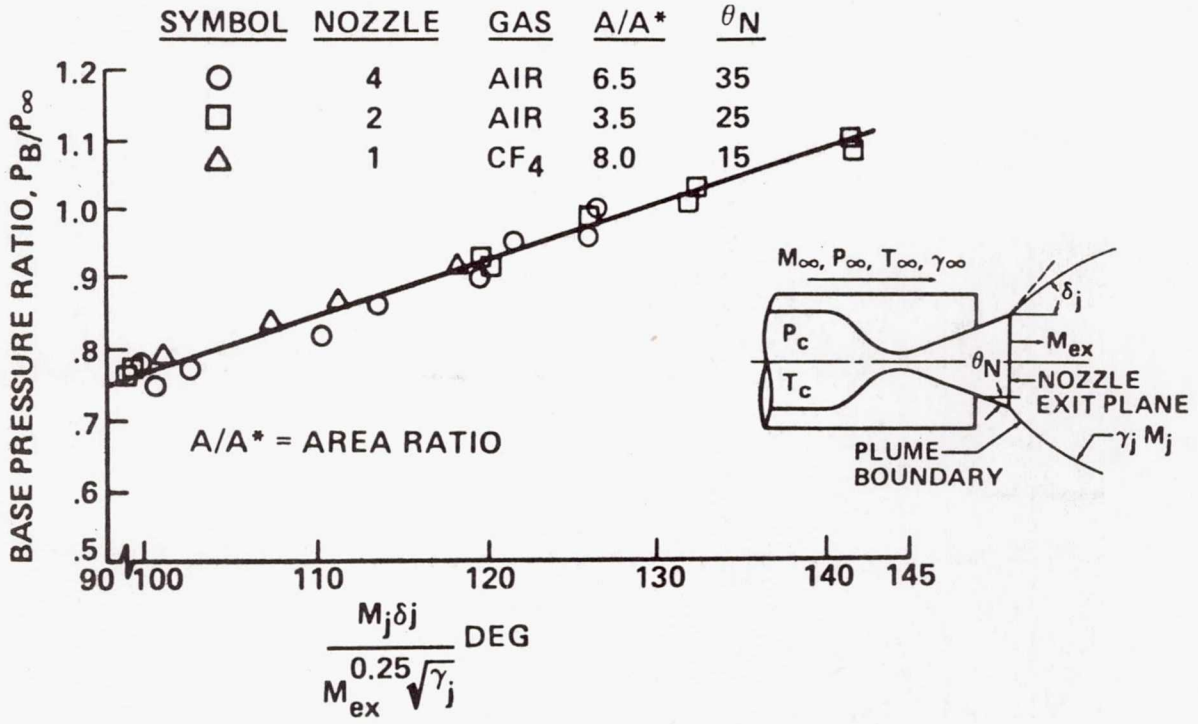

Figure 18. Example of a Successful Simulation Parameter; Cone-Cylinder Geometry.

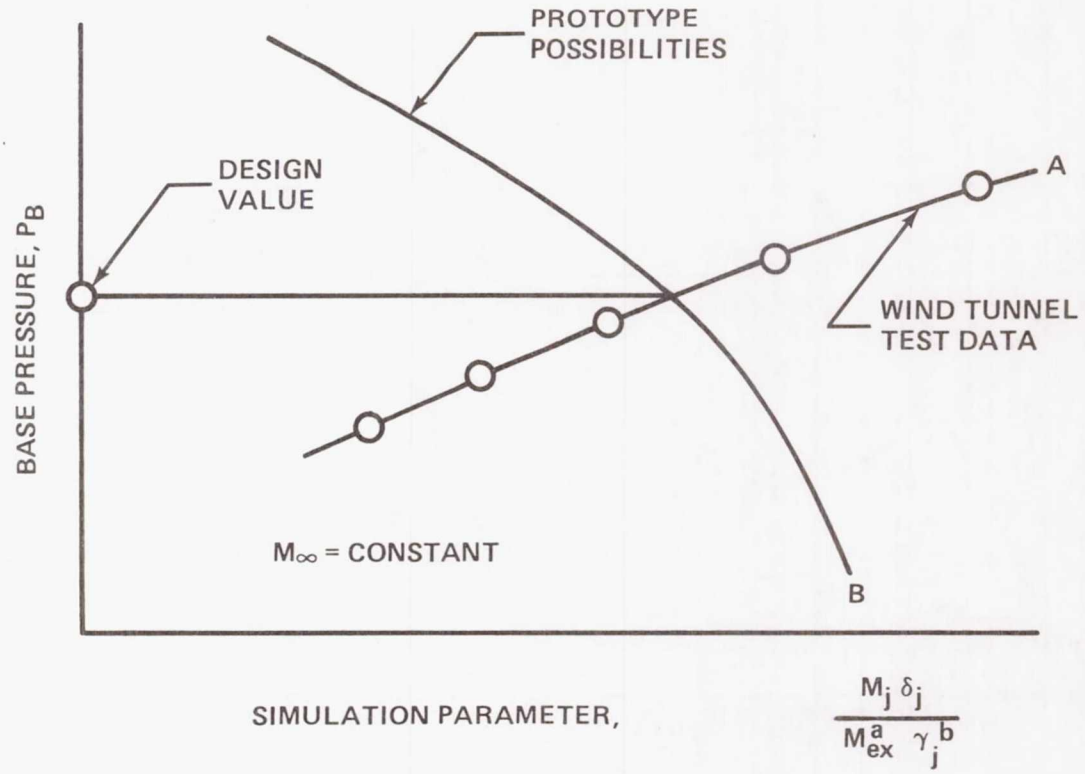

Figure 19. Application of Plume Simulation Parameters to Wind Tunnel Testing.

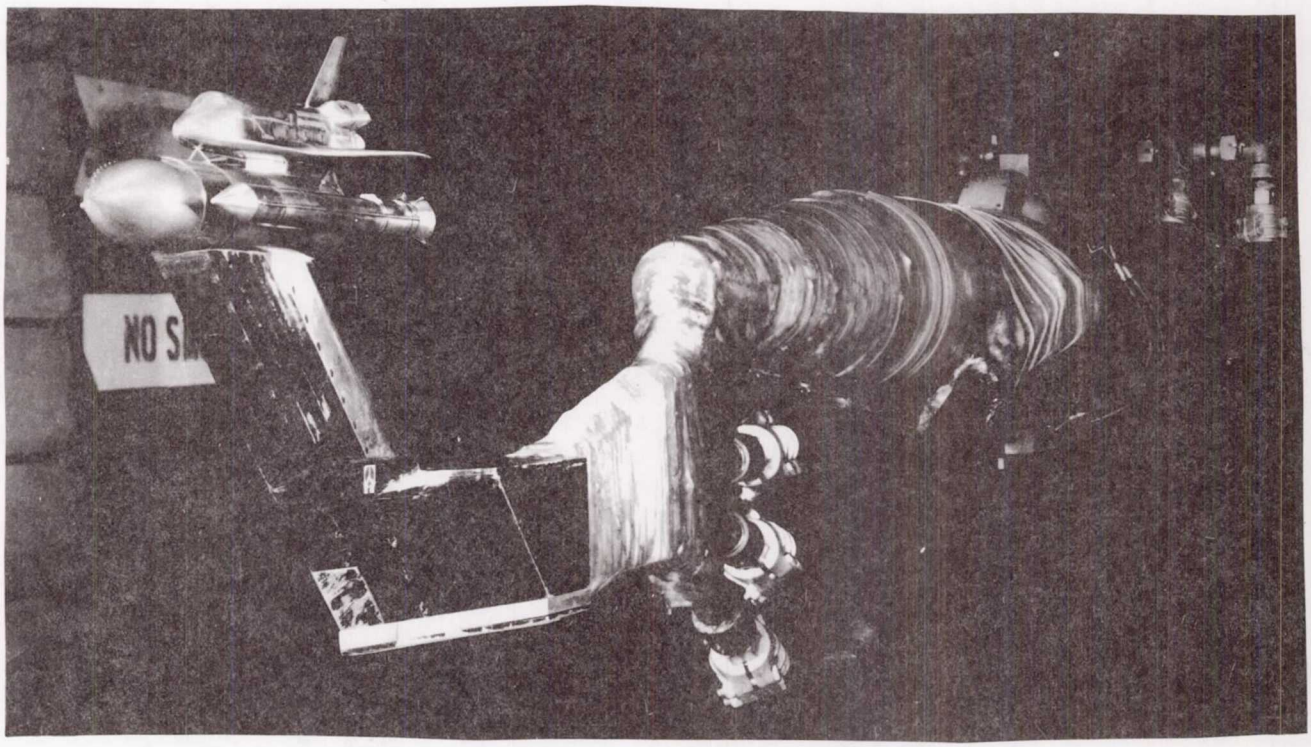

Figure 20. Launch Vehicle Plume Test Model in ARC UPWT.

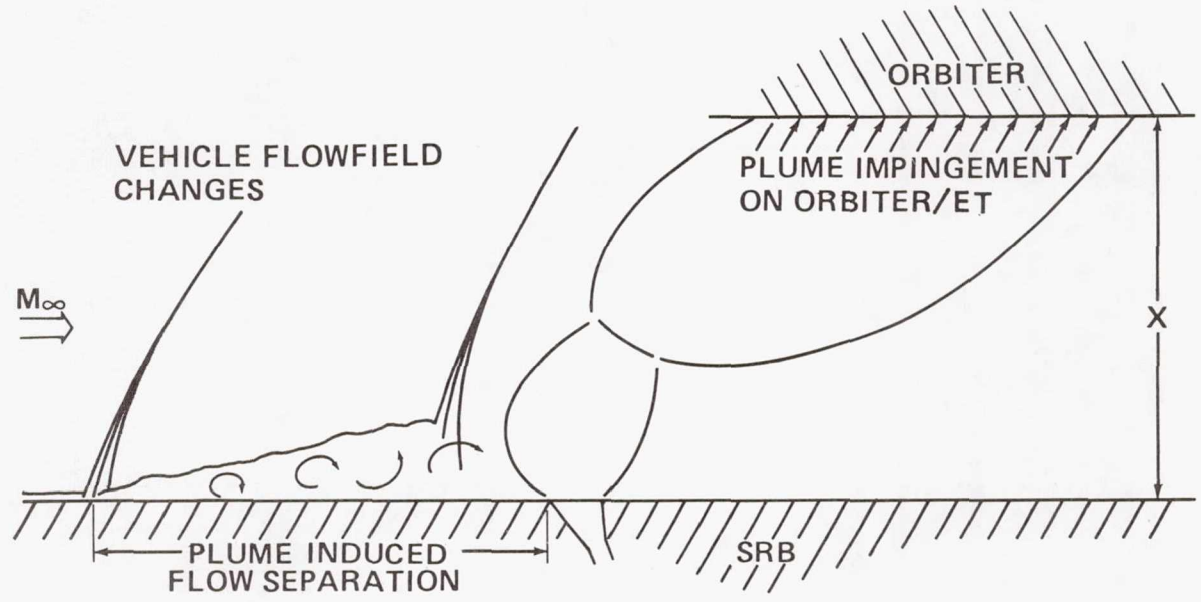

Figure 21. Schematic of BSM Plume Simulation Requirements.

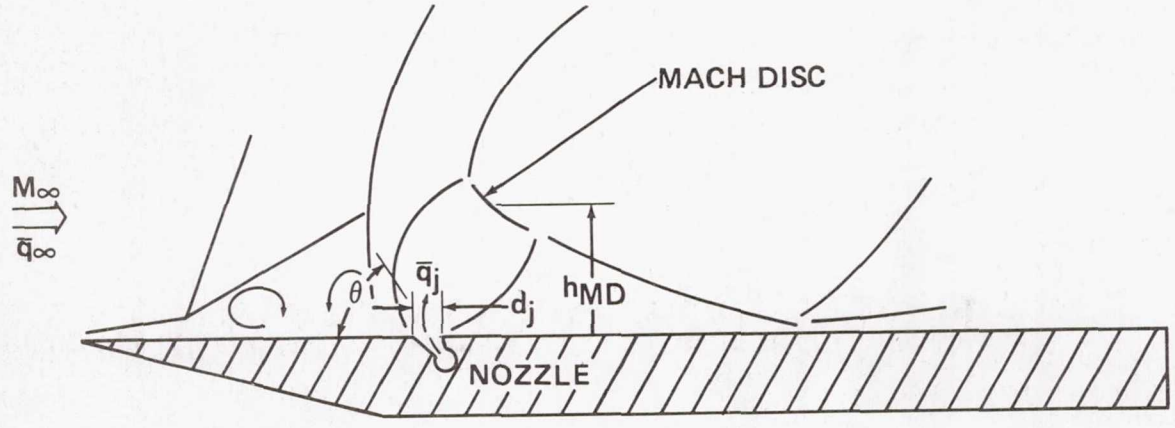

$$h_{MD}=\left[\frac{2\left(1+\frac{\gamma_j-1}{2}M_j^2\right)}{\gamma_j^2 M_j\left(\gamma_j+1\right)}\right]^{0.25}\left[\frac{1.25\left(1+\gamma_\infty\right)\gamma_\infty M_\infty^2}{\left(1-\gamma_\infty\right)+2\gamma_\infty M_\infty^2}\right]^{0.5}\left[\frac{\bar{q}_j}{\bar{q}_\infty}\right]^{0.5}\left\{\frac{d_j}{\left(1+\cos\theta_j\right)}\right\}$$

Figure 22. Transverse Firing Jet Similarity Parameter.

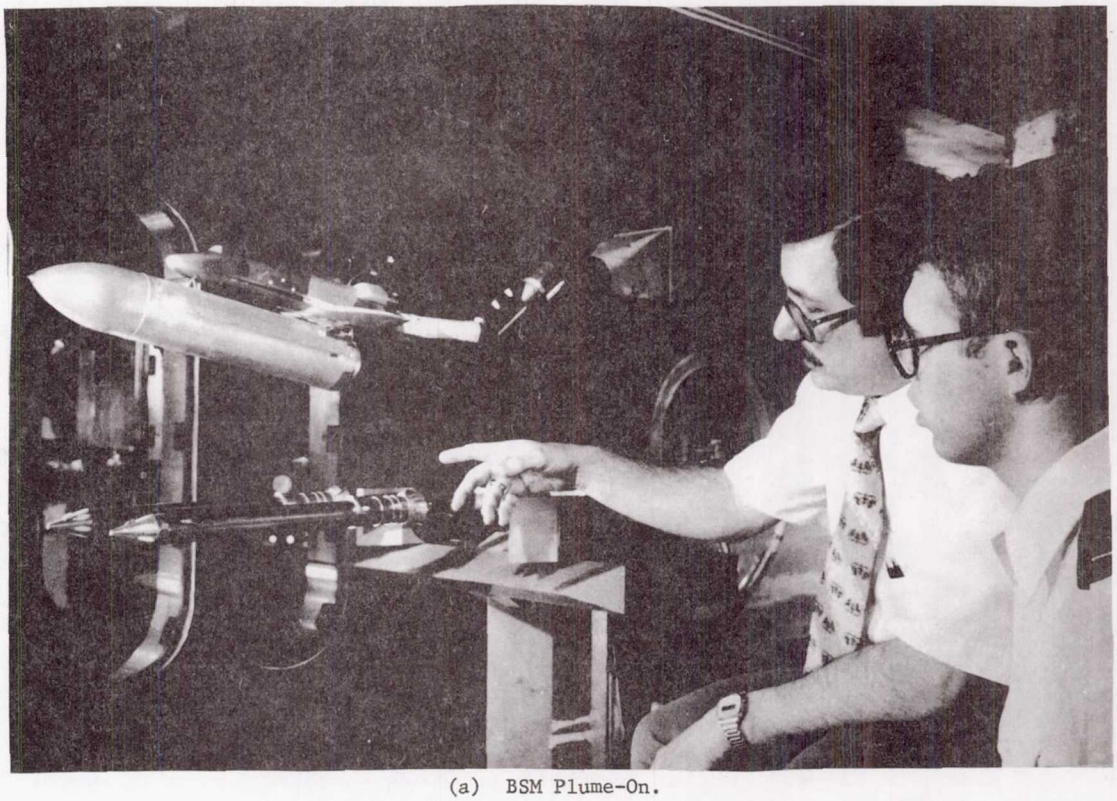

(a) BSM Plume-On.

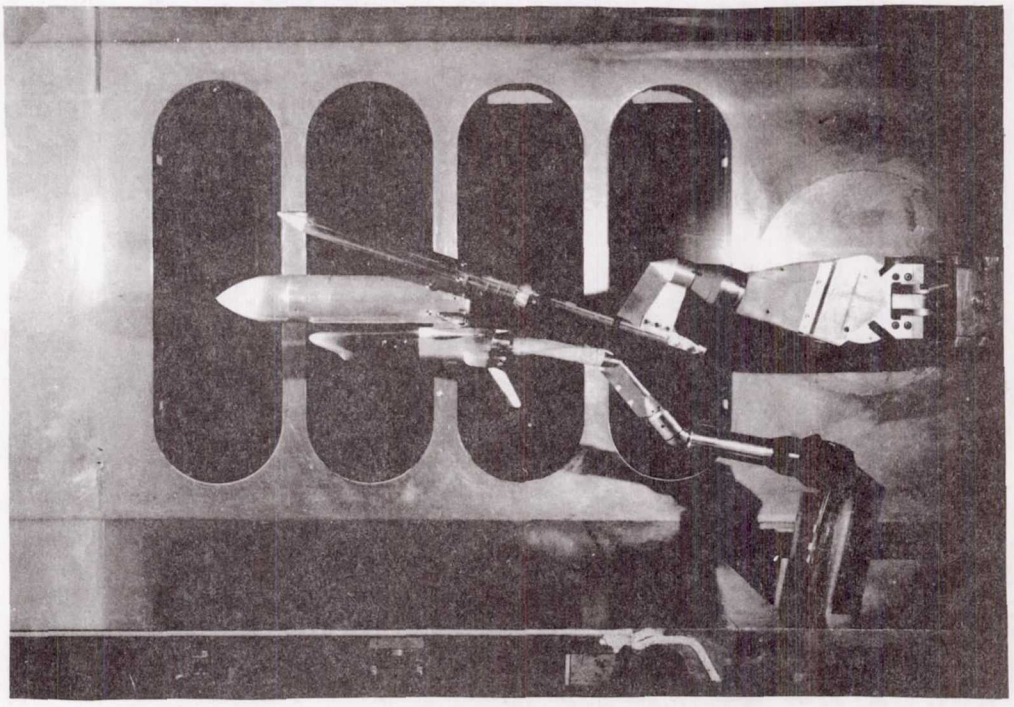

(b) BSM Plume-Off.

Figure 23. SRB Separation Test Model Installation in AEDC/VKF Tunnel A.